

ETD Archive

---

2014

## Electrostatically Controlled Enzymatic Reaction, Metabolic Processes and Microbial Generation of Electric Power

Yang Song  
*Cleveland State University*

Follow this and additional works at: <https://engagedscholarship.csuohio.edu/etdarchive>

 Part of the [Electrical and Computer Engineering Commons](#)

[How does access to this work benefit you? Let us know!](#)

---

### Recommended Citation

Song, Yang, "Electrostatically Controlled Enzymatic Reaction, Metabolic Processes and Microbial Generation of Electric Power" (2014). *ETD Archive*. 829.  
<https://engagedscholarship.csuohio.edu/etdarchive/829>

This Thesis is brought to you for free and open access by EngagedScholarship@CSU. It has been accepted for inclusion in ETD Archive by an authorized administrator of EngagedScholarship@CSU. For more information, please contact [library.es@csuohio.edu](mailto:library.es@csuohio.edu).

ELECTROSTATICALLY CONTROLLED ENZYMATIC REACTION,  
METABOLIC PROCESSES AND MICROBIAL GENERATION OF  
ELECTRIC POWER

YANG SONG

Bachelor of Electrical Engineering  
Nankai University  
July, 2011

submitted in partial fulfillment of requirements for the degree  
MASTER OF SCIENCE IN ELECTRICAL ENGINEERING  
at the  
CLEVELAND STATE UNIVERSITY  
May, 2014

We hereby approve this thesis for

Yang Song

Candidate for the Master of Science in Electrical Engineering degree for the

Department of Electrical and Computer Engineering

and the CLEVELAND STATE UNIVERSITY

College of Graduate Studies

---

Thesis Chairperson, SiuTung Yau

---

Electrical and Computer Engineering Department & Date

---

Thesis Committee Member, Fuqin Xiong

---

Electrical and Computer Engineering Department & Date

---

Thesis Committee Member, Lili Dong

---

Electrical and Computer Engineering Department & Date

Student's Date of Defense: (4/18/2014)

## **ACKNOWLEDGEMENTS**

I would like to express my sincere gratitude to Dr. SiuTung Yau, my academic advisor, for introducing me to the broad and interesting world of biosensors and nanotechnology, patiently guiding me through the entire thesis research, the opportunity to touch the edging techniques in the biosensor and microbial fuel cell.

I would like to offer my special thanks to Dr Fuqin Xiong and Dr Lili Dong for serving on my thesis committee and providing invaluable advices for my thesis.

I would like to take this opportunity to thank to Jiapeng Wang for his help in the composition of this thesis.

I would also like to thank to my family and friends for their support and encouragement throughout my study.

ELECTROSTATICALLY CONTROLLED ENZYMATIC REACTION,  
METABOLIC PROCESSES AND MICROBIAL GENERATION OF  
ELECTRIC POWER

YANG SONG

**ABSTRACT**

This thesis shows that electric fields can be used to control electron transport in biological systems and improve the performance of biological devices using an external gating voltage. It has recently been shown that an ultrasensitive detection method based on electric field effect can be used to control the kinetics of enzymatic conversion of glucose. The first part of the thesis is a mechanistic study of the enzyme catalyzed conversion of glucose to gluconolactone using the field effect enzymatic detection (FEED) technique. Use of a voltage controlled enzymatic system decreased electrons tunnel between electrode and active center of glucose oxidase (GOx) to 13mM, as compared with normal status (56mM). The catalytic constant of glucose molecules was also increased to  $870\text{S}^{-1}$ . A high concentration of PBS in the system would induce more

electrical charges which will induce a stronger electrical field. The results indicate that electrostatic field effect can be used to improve the activity of a redox enzyme immobilized on an electrode by setting up electric field on the interface.

Next, the FEED technique is applied to the metabolism of glucose by yeast cells. A transistor-like electrochemical device is constructed to control the glucose metabolism process. Finally, the FEED is used to enhance the performance of yeast-based microbial fuel cell.

# TABLE OF CONTENTS

ACKNOWLEDGEMENTS.....	III
ABSTRACT.....	IV
LIST OF FIGURES .....	VIII
CHAPTER	
I INTRODUCTION.....	1
1.1 Electrostatically controlled biological systems.....	1
1.2 FEED technique .....	1
1.3 Elucidation of FEED mechanism.....	3
1.4 Controlled glucose metabolism.....	3
1.5 Improved performance of microbial fuel cell .....	4
1.6 References .....	4
II VOLTAGE CONTROLLED ENZYME CATALYZED GLUCOSE- GLUCONOLACTONE CONVERSION.....	9
2.1 Summary .....	9
2.2 Method and Materials .....	10
2.3 Results .....	12
2.4 Discussion .....	14
2.5 References .....	16
III ELECTROSTATICALLY CONTROLLED METABOLISM OF GLUCOSE IN YEAST.....	24
3.1 Summary .....	24

3.2 Materials and methods .....	25
3.3 Results .....	27
3.4 Discussion .....	30
3.5 References .....	32
IV THE ELECTROSTATICALLY ENHANCED PERFORMANCE OF MICROBIAL FUEL CELL .....	46
4.1 Summary .....	46
4.2 Materials and methods .....	47
4.3 Result .....	49
4.4 Discussion .....	52
4.5 References .....	54
V CONCLUSIONS AND FUTURE WORK.....	61
5.1 Conclusions.....	61
5.2 Future work.....	62
5.3 References.....	63



## LIST OF FIGURES

<b>Figure</b>		<b>Page</b>
Figure 1-1:	Cross-sectional view of experimental setup .....	6
Figure 1-2:	The ion-induced electric field at the solution-electrode interface.....	7
Figure 1-3:	Energy profile of the molecule-electrode interface .....	8
Figure 2-1:	Cross-sectional view of experimental setup .....	17
Figure 2-2	Mass spectra showing the glucose – gluconolactone conversion.....	18
Figure 2-3	The $V_G$ -dependence of the glucose oxidation current.....	19
Figure 2-4	The oxidation current in different ion concentration.....	20
Figure 2-5	The effect of $V_G$ on the time-dependent depletion of glucose.....	21
Figure 2-6	$V_G$ -dependent glucose calibration curves.....	22
Figure 2-7	The $V_G$ -dependent $K_{cat}$ and $K_m$ .....	23
Figure 3-1	Electrostatically controlled system .....	34
Figure 3-2	CVs showing the yeast-induced oxidation of glucose.....	34
Figure 3-3	$V_G$ -dependent change in glucose concentration in aerobic condition.....	35
Figure 3-4	$V_G$ -dependent change in glucose concentration in anaerobic condition....	36
Figure 3-5	SEM image of yeast-immobilized electrode.....	37
Figure 3-6	$V_G$ -controlled production of ATP under the aerobic condition.....	38

Figure 3-7	$V_G$ -controlled production of ATP under the anaerobic condition.....	39
Figure 3-8	$V_G$ -controlled generation of ethanol.....	40
Figure 3-9	the change in pH under the anaerobic condition.....	41
Figure 3-10	Transfer characteristics of the metabolic transistor.....	42
Figure 3-11	The ethanol production using the two-electrode system.....	43
Figure 3-12	Glucose consumption in the two-electrode system.....	44
Figure 3-13	Scenario for electron shuttle through enzymes.....	45
Figure 4-1	Schematic description of additional electrode-anode system.....	56
Figure 4-2	CVs of yeast-immobilized electrode under different conditions.....	57
Figure 4-3	Anode potential, cathode potential and OCV.....	58
Figure 4-4	Polarization curve and power curve.....	59
Figure 4-5	Coulombic efficiency of MFC.....	60

# **CHAPTER I**

## **INTRODUCTION**

### **1.1 Electrostatically controlled biological systems**

Electron transfer (ET) is a fundamental process responsible for important biological phenomena such as photosynthesis, respiration and metabolism [1]. Effectively controlled electron transfer is one of the important regulation mechanisms in biology and biomolecular machines [2, 3], whereas efficiently controlled kinetics of biological catalysis reaction is an essential requirement for viable renewable and green energy processes [4]. Electrons in biological systems transfer between active sites, which are embedment with insulating polypeptide networks. Therefore, the rate of ET in biological systems is absolutely low [5]. Recently, an electrostatic technique has been used to control the rate of ET in different kinds of biological system.

### **1.2 FEED technique**

The technique, field-effect enzymatic detection (FEED), is based on modifying the conventional three-electrode electrochemical cell with additional gating electrodes for applying a gating voltage  $V_G$  between the gating electrode and the working electrode [5],

upon which a redox enzyme is immobilized.  $V_G$  induces an electric field that penetrates the enzyme and lowers the energy barrier between the electrode and the enzyme's active site, allowing more electrons to be transferred to result in  $V_G$ -controlled current amplification [5]. The current amplification provided by FEED has been applied to glucose biosensors to detect glucose on the zepto-molar level [6]. The research included in this thesis is on three aspects of FEED as described in the following sections.

Fig 1-1 shows the basic structure of FEED system. When the  $V_G$  is positive, the  $V_G$  will induce the ions at the interface between enzyme and solution. Fig 1-2 shows net interfacial charge distribution. The induced ions could set up electric field across activity center which is embedment with polypeptide groups [5]. The polypeptide groups result in low level of interfacial electron transfer rate between active site and electrode [9]. Fig 1-3 is the schematic description of the induced electric field forming at enzyme-electrode interface [7, 10]. When quantum state is in equilibrium, no electron can transfer between activity center and electrode, since the energy of quantum state of active site,  $E_{red}$ , is lower than the Fermi energy. The electron transfer rate ( $K_{et}$ ) depends on the distance ( $d$ ) between electrode and active site of GOx, which is shown as  $K_{et} \propto \exp(-\beta d)$  [11]. From the equation,  $K_{et}$  was also related with the attenuation coefficient,  $\beta$ , which depends on the square root of height of electron tunnel barrier. When  $V_G$  is increasing, the induced electric field can lower the effective height of electron tunnel barrier, resulting in reducing the value of attenuation coefficient  $\beta$  and enhancing electron transfer rate  $K_{et}$  [10, 11].

### **1.3 Elucidation of FEED mechanism**

In addition to providing signal amplification in biosensors, the FEED technique can be used to ET at general biological-inorganic interface. However, the mechanism of the ET process has to be studied. This research includes a series of experiments performed to elucidate the mechanism of FEED. These experiments were performed using the system of an electrode and glucose oxidase, the enzyme that catalyzes the oxidation of glucose [12]. Then, the kinetics of the enzymatic conversion of glucose to gluconolactone was characterized with  $V_G$  as the parameter [13]. The results of this study showed FEED can be used in other biological-inorganic systems.

### **1.4 Controlled glucose metabolism**

FEED has been applied to the yeast-electrode system to show the feasibility of controlling the kinetics of cellular glucose metabolic processes at the surface of an electrode. Glucose metabolism in cells generates energy for living systems to sustain biological functions [14]. Controlling cellular glucose metabolism has important implications in cancer research and synthesis of biofuels [15-17]. This work shows that the glucose consumption in yeast cells that was in contact with an electrode could be controlled by  $V_G$ . The observation that the glucose consumption qualitatively correlates to the production of the end products of glucose metabolism such as ethanol and ATP indicates that the entire process was glucose metabolism whose kinetics was controlled by applying a voltage at an insulated gating electrode. The results show a possible role for electrostatic means in several metabolism-related areas.

## 1.5 Improved performance of microbial fuel cell

Microbial fuel cell (MFCs) can convert different kind of substrate and fuel into electric power [18-21].The FEED technique was also applied to yeast-based microbial fuel cell (MFCs) to improve its performance. This work shows that applying a gating voltage to the anode of a MFC where yeast is immobilized enhances the ET into the anode so that the performance of the MFC in terms of the open-circuit voltage (OCV), the polarization curve and the power curve was improved. Since the improved performance did not occur at the cost of extra energy spent on the fuel cell, the electrostatic method appears to be a viable way to boost up the output of MFCs. The method is applicable to generic MFCs. This work indicates that the applied voltage functions as an additional operation parameter and should be considered in the design of biofuel cells.

## 1.6 References

- [1] Vélot C, Sreere P A. Reversible Transdominant Inhibition of a Metabolic Pathway IN VIVO EVIDENCE OF INTERACTION BETWEEN TWO SEQUENTIAL TRICARBOXYLIC ACID CYCLE ENZYMES IN YEAST[J]. *Journal of biological chemistry*, 2000, 275(17): 12926-12933.
- [2] Onuchic, J. N.; Kobayash, C.; Miyashita, O.; Jennings, P.; Baldrige, K. K., *Phil. Trans. R. Soc. B* 2006, 361, 1439–1443.
- [3] Nocek, J. M.; Zhou, J. S.; Forest, S. D.; Priyadarshy, S.; Beratan, D. N.; Onuchic, J. N.; Hoffman, B. M., *Chem. Rev.* 1996, 96, 2459-2489.

- [4] Alcalde, M.; Ferrer, M.; Plou, F. J.; Ballesteros, A., *Trends Biotechnol.* 2006, 24, 281-287.
- [5] Choi Y, Yau S T. Field-Effect Enzymatic Amplifying Detector with Picomolar Detection Limit[J]. *Analytical chemistry*, 2009, 81(16): 7123-7126.
- [6] Choi Y, Yau S T. Ultrasensitive biosensing on the zepto-molar level[J]. *Biosensors and Bioelectronics*, 2011, 26(7): 3386-3390.
- [7] Choi Y, Yau S T. Field-Effect Enzymatic Amplifying Detector with Picomolar Detection Limit[J]. *Analytical chemistry*, 2009, 81(16): 7123-7126.
- [8] Choi Y, Yau S T. Ultrasensitive biosensing on the zepto-molar level[J]. *Biosensors and Bioelectronics*, 2011, 26(7): 3386-3390.
- [9] Choi Y, Yau S T. Field-Effect Enzymatic Amplifying Detector with Picomolar Detection Limit[J]. *Analytical chemistry*, 2009, 81(16): 7123-7126.
- [10] Tans S J, Verschueren A R M, Dekker C. Room-temperature transistor based on a single carbon nanotube[J]. *Nature*, 1998, 393(6680): 49-52.
- [11] J. D. Jackson, *Classical Electrodynamics*, John Wiley & Sons, Danvers, 1998.
- [12] Wilson R, Turner A P F. Glucose oxidase: an ideal enzyme[J]. *Biosensors and Bioelectronics*, 1992, 7(3): 165-185.
- [13] Yau S T, Xu Y, Song Y, et al. Voltage-controlled enzyme-catalyzed glucose-gluconolactone conversion using a field-effect enzymatic detector[J]. *Physical Chemistry Chemical Physics*, 2013, 15(46): 20134-20139.
- [14] Zhao Y, Butler E B, Tan M. Targeting cellular metabolism to improve cancer therapeutics[J]. *Cell death & disease*, 2013, 4(3): e532.
- [15] Davies P, Demetrius L A, Tuszynski J A. Implications of quantum metabolism and natural selection for the origin of cancer cells and tumor progression[J]. *AIP advances*, 2012, 2(1): 011101.
- [16] Osyczka A, Moser C C, Daldal F, et al. Reversible redox energy coupling in electron transfer chains[J]. *Nature*, 2004, 427(6975): 607-612.
- [17] Nevoigt E. Progress in metabolic engineering of *Saccharomyces cerevisiae*[J]. *Microbiology and Molecular Biology Reviews*, 2008, 72(3): 379-412.
- [18] Logan B E. Peer reviewed: extracting hydrogen and electricity from renewable resources[J]. *Environmental science & technology*, 2004, 38(9): 160A-167A.
- [19] Liu H, Ramnarayanan R, Logan B E. Production of electricity during wastewater treatment using a single chamber microbial fuel cell[J]. *Environmental science & technology*, 2004, 38(7): 2281-2285.
- [20] Min B, Kim J R, Oh S E, et al. Electricity generation from swine wastewater using microbial fuel cells[J]. *Water research*, 2005, 39(20): 4961-4968.
- [21] Bond D R, Lovley D R. Electricity production by *Geobacter sulfurreducens* attached to electrodes[J]. *Applied and environmental microbiology*, 2003, 69(3): 1548-1555.

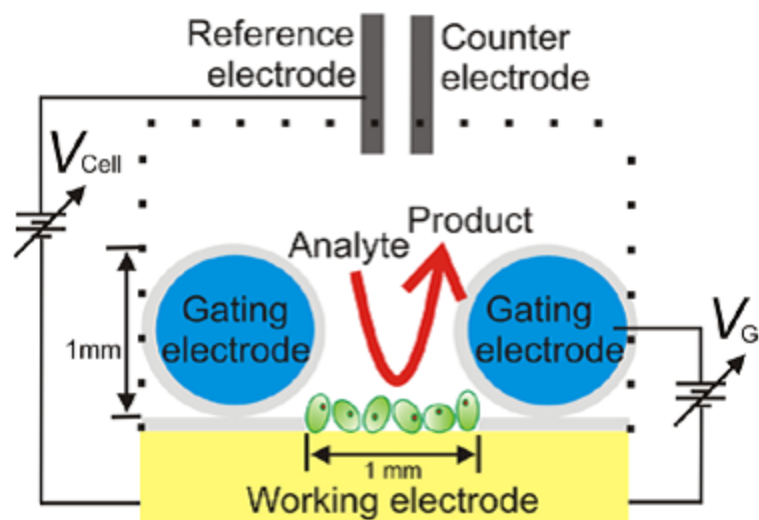


Fig 1-1 Cross-sectional view of experimental setup. Redox molecule whose active center is showed by the small point inside a molecule, is immobilized on the working electrode. The gating electrodes are represented by the circular structures, which consist of a copper wire (the blue circles) and a thin layer of insulator (the shaded shells) (Choi and Yau, 2009).



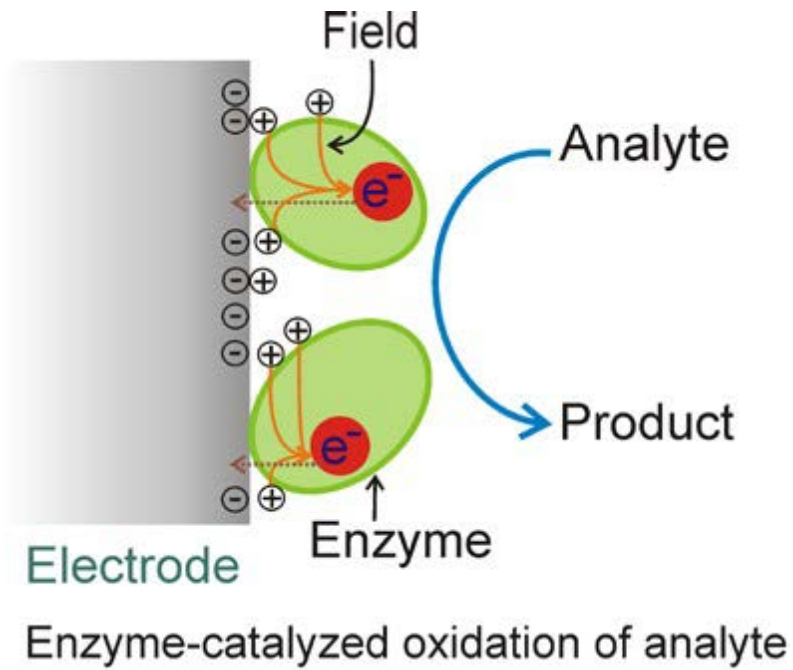


Fig 1-2 ion-formed electric field at connector between enzyme and acceptor. The brown arrow indicates the direction of electron transfer and the red arrow indicates the direction of the induced electric field(Choi and Yau,2009)

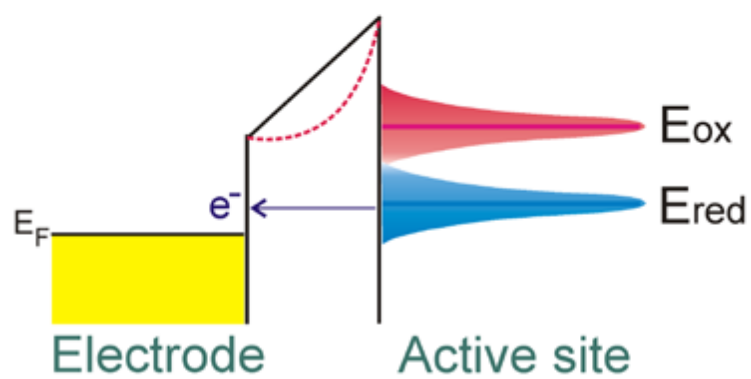
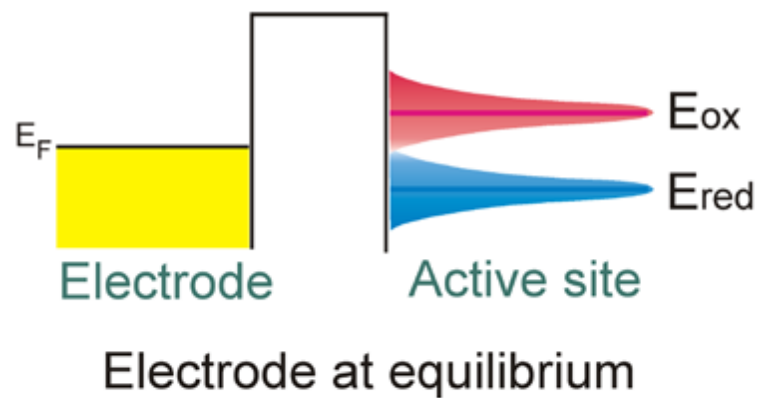


Fig 1-3 Energy state of interface between enzyme and electrode.  $E_{red}$  and  $E_{ox}$  are respectively the most probable energies for the occupied and unoccupied quantum states of the active site (Tans and Verschueren, 1998).

## **CHAPTER II**

### **VOLTAGE CONTROLLED ENZYME CATALYZED GLUCOSE- GLUCONOLACTONE CONVERSION**

#### **2.1 Summary**

A detailed study on the voltage-controlled enzymatic catalysis of the glucose-gluconolactone conversion using the FEED technique has been performed. The conversion of glucose to gluconolactone occurring at an enzyme-immobilized working electrode was confirmed using mass spectrometry. Electrochemical studies showed that the glucose oxidation current depends on the gating voltage  $V_G$  and the ion concentration of the sample solution. Additionally, the depletion of glucose in the sample also showed a dependence on  $V_G$ . FEED was used to detect  $H_2O_2$  on the zepto-molar level in order to show that the ultrasensitive detection capability is a general feature of the technique. These results, while providing evidence for the proposed mechanism of FEED, indicate that  $V_G$  controls the conversion process. The effect of  $V_G$  on the glucose-gluconolactone conversion was demonstrated by the observed  $V_G$ -dependent kinetic parameters of the conversion process. The results of our electrochemical measurements, while being used to elucidate the mechanism of FEED, provide insights into the kinetics of the conversion.

It was shown that the conversion kinetics could be manipulated using a gating voltage.

## 2.2 Method and Materials

### 2.2.1 Detection system and operation

Fig 2-1 showed the schematic field effect detector system layout. This system is made with three electrode electrochemical cell which is modified by a gating electrode [1]. The gating electrode is used to apply  $V_G$  to the working electrode where immobilized redox enzymes. Pyrolysis graphite electrode (PG, GE Advanced coop) was used as the working electrode which had an area of 0.5mm\*0.5mm and coating with mask. The GOx immobilized electrodes were prepared by deposited one drop (1mL) of GOx (Sigma Aldrich) on the PG electrode surface and incubated at 27°C for 5 hours, and then washed by demonized water. Then dry them at 27°C. The enzyme immobilization method can be used for glucose oxidase or MP-11[2], which suggests that the activity of glucose oxidase can be preserved through this method. Cyclic voltammetry was performed using GOx immobilized electrode to show  $V_G$  effect on GOx induced oxidation of glucose. A conventional three electrode cell was powered by the Cyclic Voltammetry measurement (CH660C). An Ag/AgCl electrode functioned as reference electrode and platinum wire was used as counter electrode. The gating electrode, which was made of 0.5 mm diameter copper wire with an insulator thin, have formed a U-turn structure and was attached to the surface of working electrode in order to suspend the molecules of GOx. The scan rate of the Cyclic Voltammetry system was set as 25mV/s and every detection experiments must be processed for at least five times to reach a reliable result. All the experiments were carried out at 27°C.

### **2.2.2 Reagents**

GOx (EC 1.1.3.4) and D(+)-glucose were purchased from Sigma Aldrich. All the chemicals were analytical grade without any purification. Deionized water was obtained using a Direct-Q™5 Millipore system. Phosphate buffer solution (PBS) was prepared using deionizer water and diluted with  $\text{KH}_2\text{PO}_4$  and  $\text{Na}_2\text{HPO}_4$ , then was adjusted PH with 0.1M  $\text{H}_3\text{PO}_4$  and NaOH. GOx was dissolved in 0.1M PBS and concentration was 10mg/ml.

### **2.2.3 Mass spectrometry and Glucose Meter**

Mass spectrometry experiments were performed using GOx immobilized electrode with glucose solution under chronoamperometry model at 0.8V potential. The electrospray ionization mass spectrometric experiments were conducted to analyze glucose samples with an applied bio-system (Foster City, CA) Q-Star Elite TOF mass spectrometer and with the TurboIon spray source equipment. Glucose samples, which contained the same amount of glucose and C-13 labeled heavy isotope, were diluted with same volume of 10% ammonium acetate and 90% acetonitrile. The equipment injected glucose sample at a consent rate ( $10\text{mL}/\text{min}^{-1}$ ). The data was analyzed using the software from the Analysis bio-system program. The Breeze Glucose Meter integrated with test strips, one kind of commercial blood glucose devices for measuring the glucose concentration in the blood sample, was used to measure the glucose concentration in our experiments. The measuring range of this particular instrument is  $20\text{-}650\text{mgdL}^{-1}$ .

## 2.3 Results

### 2.3.1 Mass spectrometry results

Fig 2-2(a) has shown the mass spectrometry results of glucose samples. The mass and charge ratios ( $m/z$  ratios) of deprotonated glucose and deprotonated heavy isotopes equal to 179 and 185, respectively. Fig 2-2(b) shows the results of mass spectrometry after 300s of chronoamperometry. The  $m/z$  ratios of gluconic acid and acid of heavy isotope are 195 and 201, with the intensity height 600 and 700, respectively. Additionally, the intensity height of glucose line and heavy isotope line decreased from 5000 to 2500. Thus, the result of mass spectrometry showed that glucose-gluconolactone conversion did happen at GOx immobilized electrode.

### 2.3.2 Electrostatically controlled glucose oxidization current

The process of glucose-gluconolactone conversion process is attributed to oxidation of glucose catalyzed by GOx. These stable glucose oxidation currents are due to the redox of active site of GOx [3, 4]. The results of Cyclic Voltammetry measurements (CVs) were shown by Fig 2-3. CV1, CV2 and CV3 are the currents of control experiments got in the bare electrodes in 10mM glucose with  $V_G=0V$ , 0.1V and -0.1V. CV4 is the glucose oxidation current with  $V_G=0V$  in the 10mM glucose solution. These stable glucose oxidation currents were to the results of oxidation glucose of GOx. And CV5, CV6 and CV7 are the glucose oxidization currents in 10mM glucose solution with different values of  $V_G$ . CV5 and CV6 indicate that the glucose oxidation current increased progressively when positive value of  $V_G$  was increasing. However, CV7 shows that glucose oxidation current became less than CV4 when the polarity of  $V_G$  was reversed. The increase in glucose oxidation current was attributed to the reducing height

of electron tunnel barrier [5-6], whereas the decreasing in glucose oxidation current was due to increase height of electron tunnel barrier.

The  $V_G$  dependent glucose oxidation currents in different ion concentration of PBS (Fig 2-4) provided more evidence for mechanism shown in Fig 1-2 and Fig 1-3. The CV2 and CV3 can show the glucose oxidation current happened progressively increasing when concentration of PBS was increased. The increasing glucose oxidation currents are due to the fact that induced ions on the enzyme-solution interface can set up electric field to control height of electron tunnel barrier. As the ion concentration of PBS was increasing, more ions were induced to set up stronger electrical field, resulting in a lower height of electron tunnel barrier.

### **2.3.3 FEED controlled glucose consumption**

Fig 2-5 shows the glucose concentration changing at different value of  $V_G$  under aerobic condition using GOx immobilized electrode. Curve-1 shows the gradual decreasing in glucose concentration during the period of 700s at  $V_G=0V$ , which decreased by 14% of the initial glucose and used as reference one. Curve-2 to curve-5 suggested that with the increasing positive value of  $V_G$ , the glucose consumption rate will increase gradually at first and then will approach to a constant rate.

Curve-6 and curve-7 proves that the glucose consumption rate will slower down with a negative  $V_G$ . This trend also corresponds to the theoretical mechanism shown in Fig1-2 and Fig1-3.

The different glucose consumption rates indicate that the speed of glucose-gluconolactone catalyzed conversion can be controlled by  $V_G$ .

### 2.3.4 FEED controlled glucose calibration curves for different glucose concentration

Fig 2-6 shows the  $V_G$  dependent glucose calibration curves obtained from the anodic/oxidation current on the CVs at 0.8V under different values of  $V_G$  by using GOx immobilized electrode in different concentration of glucose solution. The current roughly changes as a linear response to the glucose concentrations. The nonlinearity is probably the result of enzymatic reaction under close-saturation kinetics condition.

## 2.4 Discussion

It can be predicted that  $V_G$  induced ions could set up electric field at enzyme-solution interface from the observation of the  $V_G$  dependent glucose oxidation current corresponding to the ion concentration of PBS. In order to exhibit electrostatically effect on glucose oxidation on GOx immobilization electrode, the  $V_G$  controlled kinetics of glucose-gluconolactone conversion processes were estimated by  $V_G$  dependent glucose calibration curves in Fig 2-6. The two kinetics constants of glucose-gluconolactone conversion can be changed by  $V_G$  (Fig2-7). Therefore, the kinetics of glucose-gluconolactone conversion will be influenced by  $V_G$ .

There are two parameters involved in the kinetics of the glucose-gluconolactone conversion happened at enzyme-electrode interface,  $K_{cat}$  and  $K_m$  [7].  $K_{cat}$ , the turnover number is the maximum number of substrate converted per second per active center; whereas  $K_m$  is the Michaelis constant indicating the amount of glucose for the half conversion speed [7]. Since  $K_m$  is obtained by GOx immobilized electrode, it indicates the catalytic efficiency of GOx immobilized on electrode. The lineweaver-burk equation

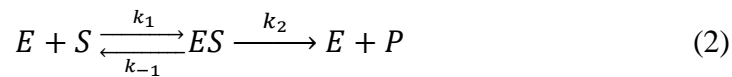


[8] is shown as,

$$1/I_{ox} = \{k'_m/(nFAk_{cat}\Gamma[glucose]) + 1/nFAk_{cat}\Gamma\} \quad (1)$$

Where,  $I_{ox}$  is the glucose oxidation current measured at  $V_{cell}=0.8V$ ,  $F$  is Faraday constant,  $n$  is electron transfer in the reaction,  $\Gamma$  is the electrode's surface coverage by GOx and  $A$  is the electrode surface area. As  $1/I_{ox}$  is a linear dependence on  $1/[glucose]$ , the  $K_{cat}$  and  $K_m$  are obtained from the slop and vertical intercept of lineweaver-burk equation. The number of electron transfer in the reaction,  $n$  can be obtained using Laviron Equation,  $I_{ox} = (nFQv) / (4RT)$ , where  $Q$  is the charge of an electron,  $v$  is electrochemistry scan rate and  $F$  is Faraday constant [8]. So  $\Gamma$  can be estimated by using the equation  $\Gamma = (4I_{ox}RT) / (n^2F^2Av)$  at room temperature with  $v=25VS^{-1}$  and  $n=2.2$  [9]. By using  $1mm^2$  of electrode surface area,  $T$  can be calculated to be  $1.125 \times 10^{-11} \text{ molcm}^{-2}$ . The value of  $T$  is shown the one monolayer layer as the size of glucose oxidase is  $6 \times 5.2 \times 7.7 \text{ nm}$ .

As  $V_G$  is increasing,  $K_{cat}$  increases while  $K_m$  decreases (Fig 2-7). Generally, enzyme catalyze reaction can be shown as



Where,  $E$  is GOx,  $S$  is glucose,  $ES$  is the enzyme-substrate complex and  $P$  is the final product [9]. As the final step is the catalytic process, enzyme will be recovered to normal site after  $P$  is formed. The  $V_G$  could accelerate the GOx-catalyzed glucose-gluconolactone conversion (Fig2-7), because electron transfer would happen as the second step [10]. The electron transfer rate ( $K_{et}$ ) will be enhanced due to  $V_G$  induced electric field, which leads to a higher  $K_{cat}$  ( $K_2$ ) contributing to more glucose conversion into gluconolactone at the second step. This will enhance the next conversion step.

Therefore, the glucose concentration for half of maximum speed will be lowered indicating a higher bio-catalytic efficiency. This capability is useful for other bio-devices.

## 2.5 References

- [1] Choi Y, Yau S T. Field-Effect Enzymatic Amplifying Detector with Picomolar Detection Limit[J]. *Analytical chemistry*, 2009, 81(16): 7123-7126.
- [2] Choi Y, Yau S T. Ultrasensitive biosensing on the zepto-molar level[J]. *Biosensors and Bioelectronics*, 2011, 26(7): 3386-3390.
- [3] Shi W, Ma Z. Amperometric glucose biosensor based on a triangular silver nanoprisms/chitosan composite film as immobilization matrix[J]. *Biosensors and Bioelectronics*, 2010, 26(3): 1098-1103.
- [4] Chen Y, Li Y, Sun D, et al. Fabrication of gold nanoparticles on bilayer graphene for glucose electrochemical biosensing[J]. *Journal of Materials Chemistry*, 2011, 21(21): 7604-7611.
- [5] Choi Y, Yau S T. Field-Effect Enzymatic Amplifying Detector with Picomolar Detection Limit[J]. *Analytical chemistry*, 2009, 81(16): 7123-7126.
- [6] Tans S J, Verschueren A R M, Dekker C. Room-temperature transistor based on a single carbon nanotube[J]. *Nature*, 1998, 393(6680): 49-52.
- [7] Kamin R A, Wilson G S. Rotating ring-disk enzyme electrode for biocatalysis kinetic studies and characterization of the immobilized enzyme layer[J]. *Analytical Chemistry*, 1980, 52(8): 1198-1205.
- [8] Lineweaver H, Burk D. The determination of enzyme dissociation constants[J]. *Journal of the American Chemical Society*, 1934, 56(3): 658-666.
- [9] Choi Y, Yau S T. Field-controlled electron transfer and reaction kinetics of the biological catalytic system of microperoxidase-11 and hydrogen peroxide[J]. *AIP Advances*, 2011, 1(4): 042175.
- [10] Honeychurch M J, Hill H A O, Wong L L. The thermodynamics and kinetics of electron transfer in the cytochrome P450<sub>cam</sub> enzyme system[J]. *FEBS letters*, 1999, 451(3): 351-353.

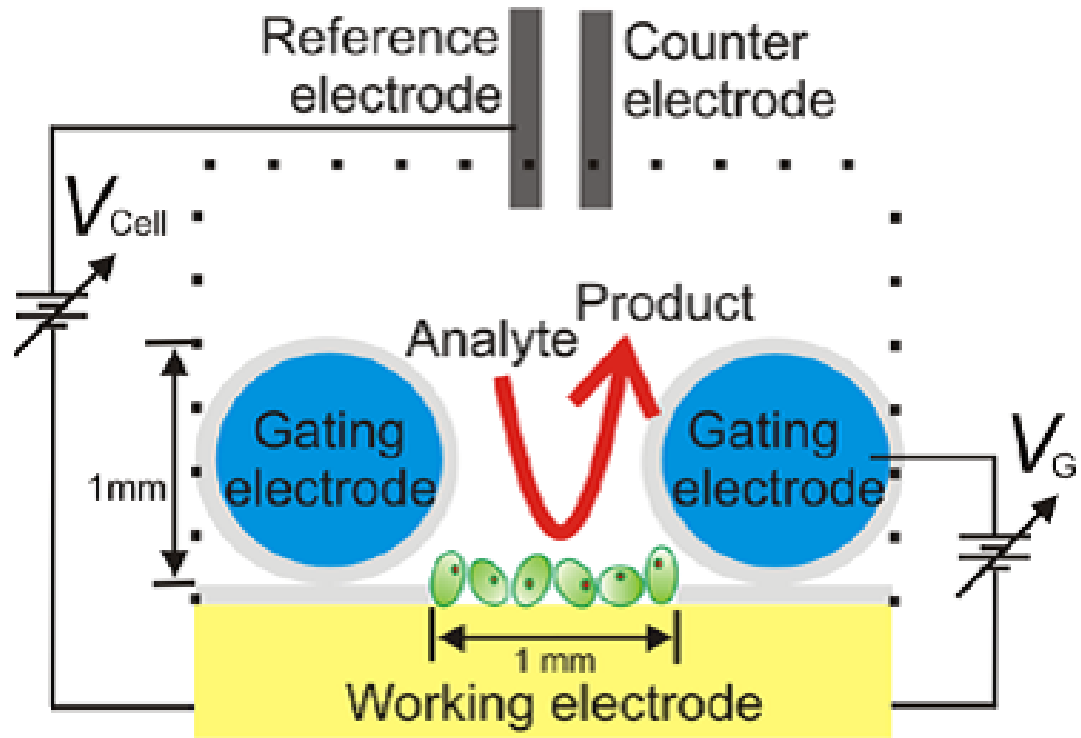


Fig 2-1 Cross-section view of experimental setup (Choi and Yau, 2009).

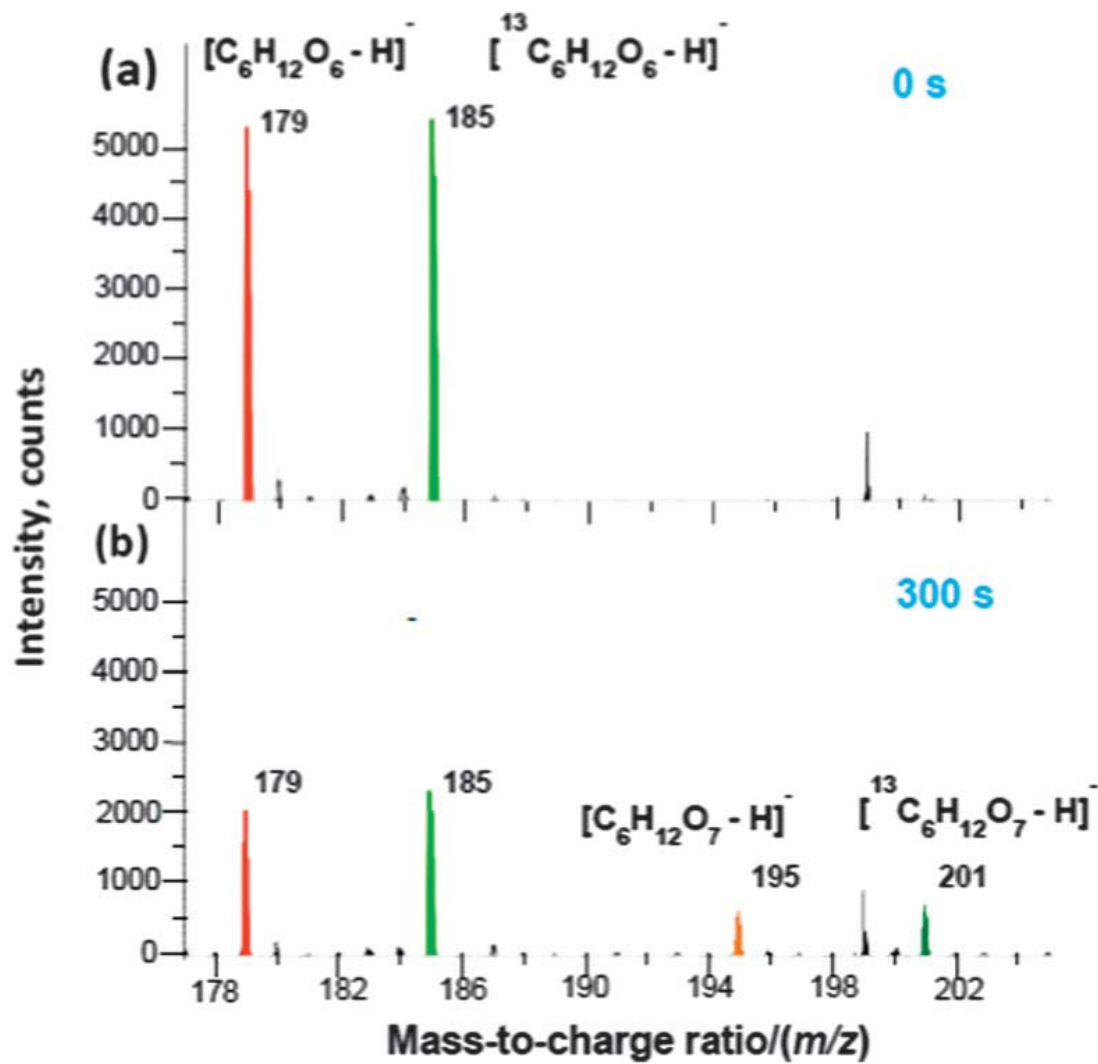


Fig 2-2 Mass spectra showing the glucose - gluconolactone conversion. (a) A spectrum showing glucose and  $^{13}\text{C}_6$ -glucose at  $t=0$ s. (b) decreasing in glucose and  $^{13}\text{C}_6$ -glucose and production of enzymatic reaction at  $t=300$ s (Yau, Xu and Song, 2013).

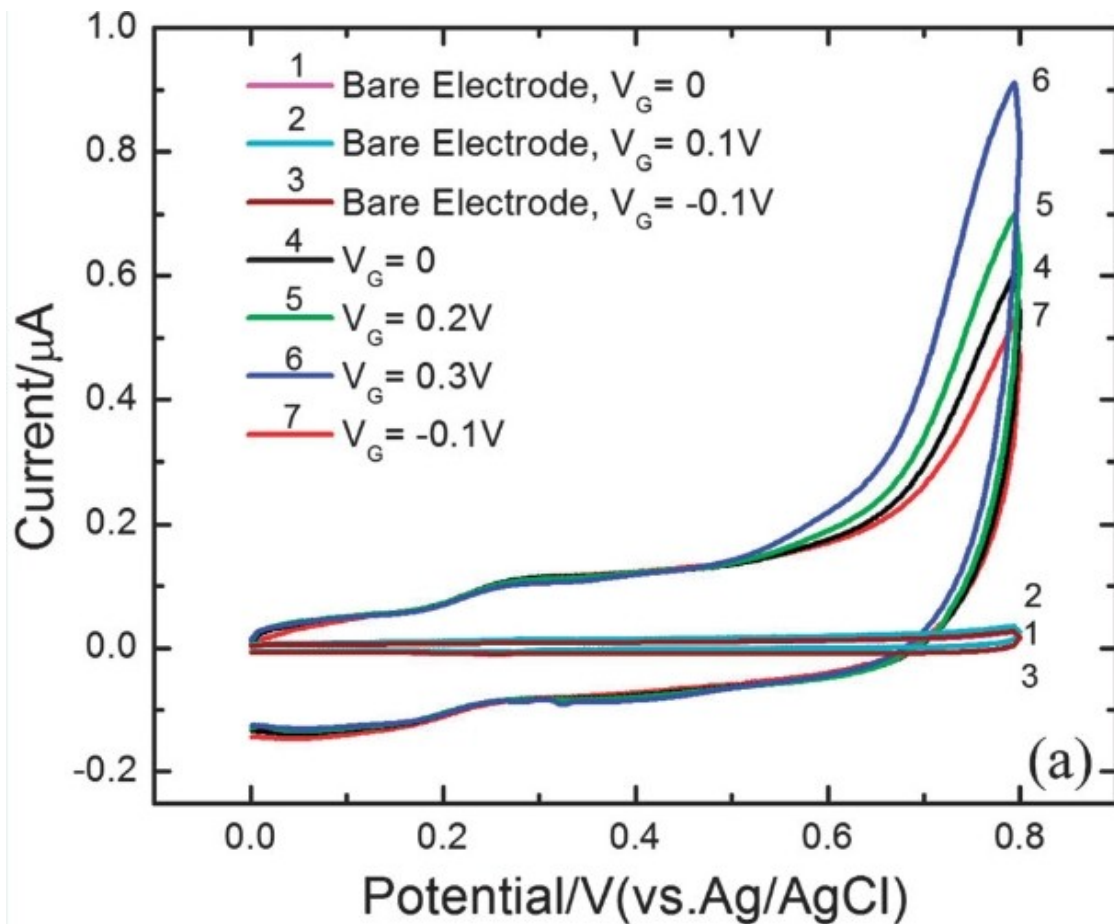


Fig 2-3 The  $V_G$ -dependence of the glucose oxidation current in 10 mM PBS. CVs obtained using GOx immobilized electrode with glucose solution under different conditions (Yau, Xu and Song, 2013).

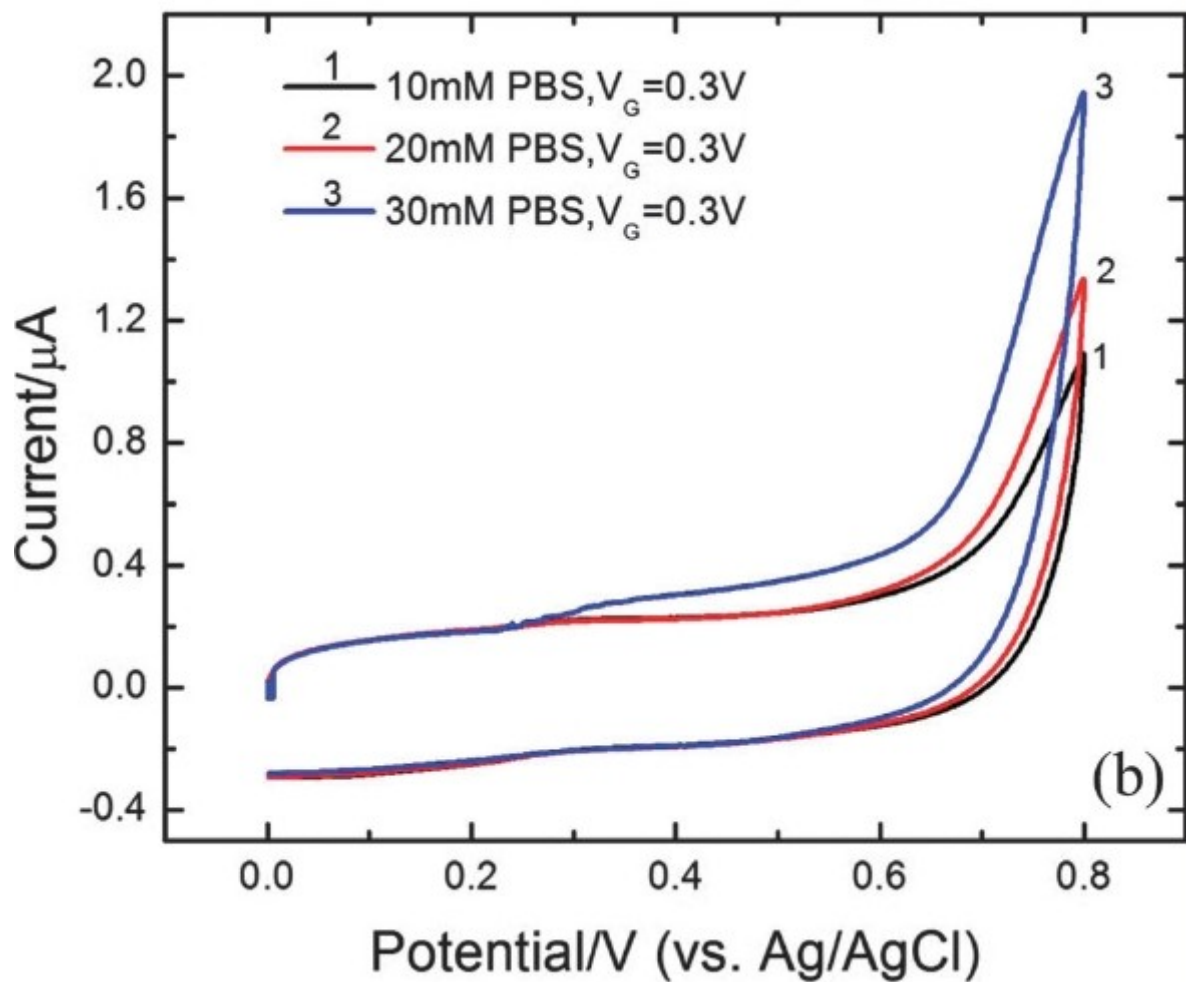


Fig 2-4 The oxidation current in different ion concentration. CVs were obtained with  $V_G = 0.3\text{V}$  by using GOx immobilized electrode in presented of different concentration of PBS and 10mM glucose (Yau, Xu and Song, 2013).

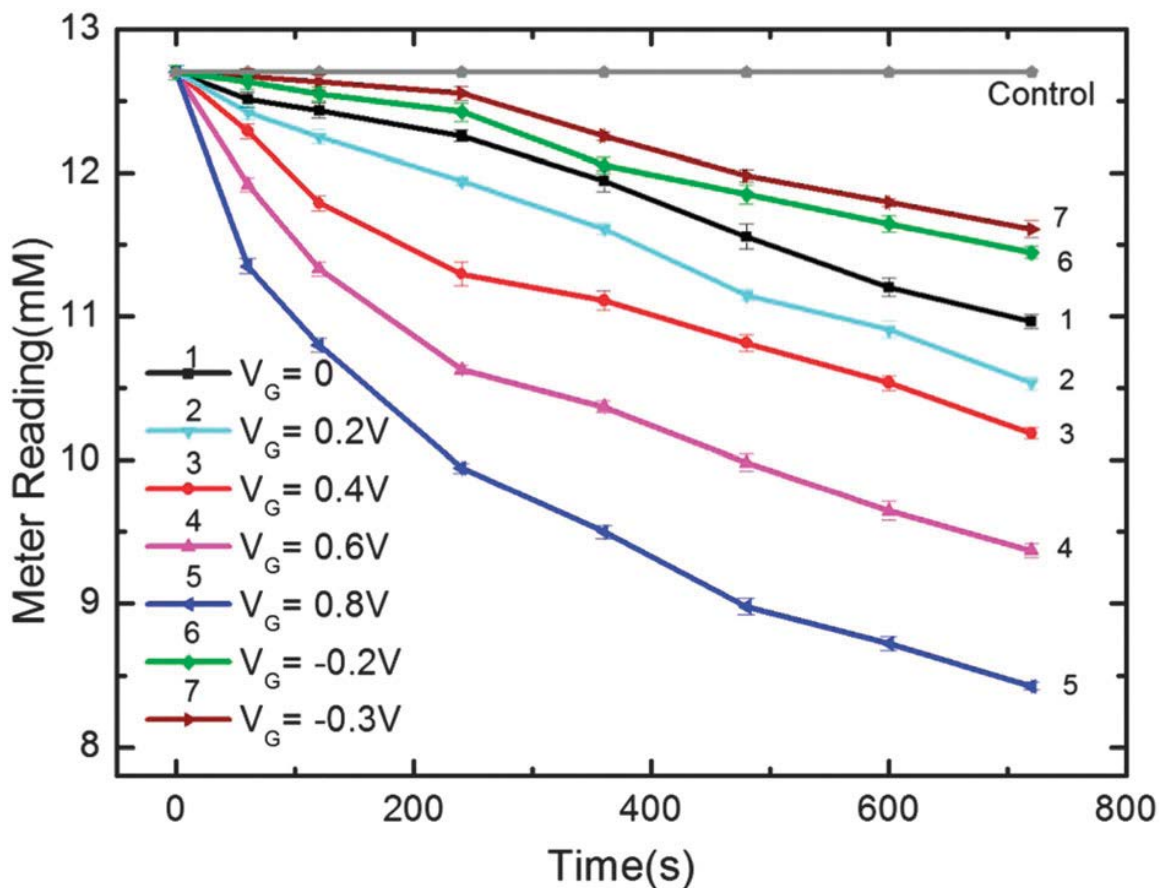


Fig 2-5 The effect of VG on the time-dependent depletion of glucose in the sample (Yau, Xu and Song, 2013). The samples of glucose solution (12.7mM) were processed using the electrochemistry system in Fig 2-1(a) at  $V_{cell}=0.8V$  vs. Ag/AgCl for a total time of 700s. The measurements of the glucose concentration were performed with glucose meter. The control experiment was set up using blank graphite electrode. Positive  $V_G$  can reduce the effective height of electron tunnel barrier, resulting in high speed of conversion of glucose. The negative  $V_G$  can increase height of electron tunnel barrier, result in slow down the speed of conversion.

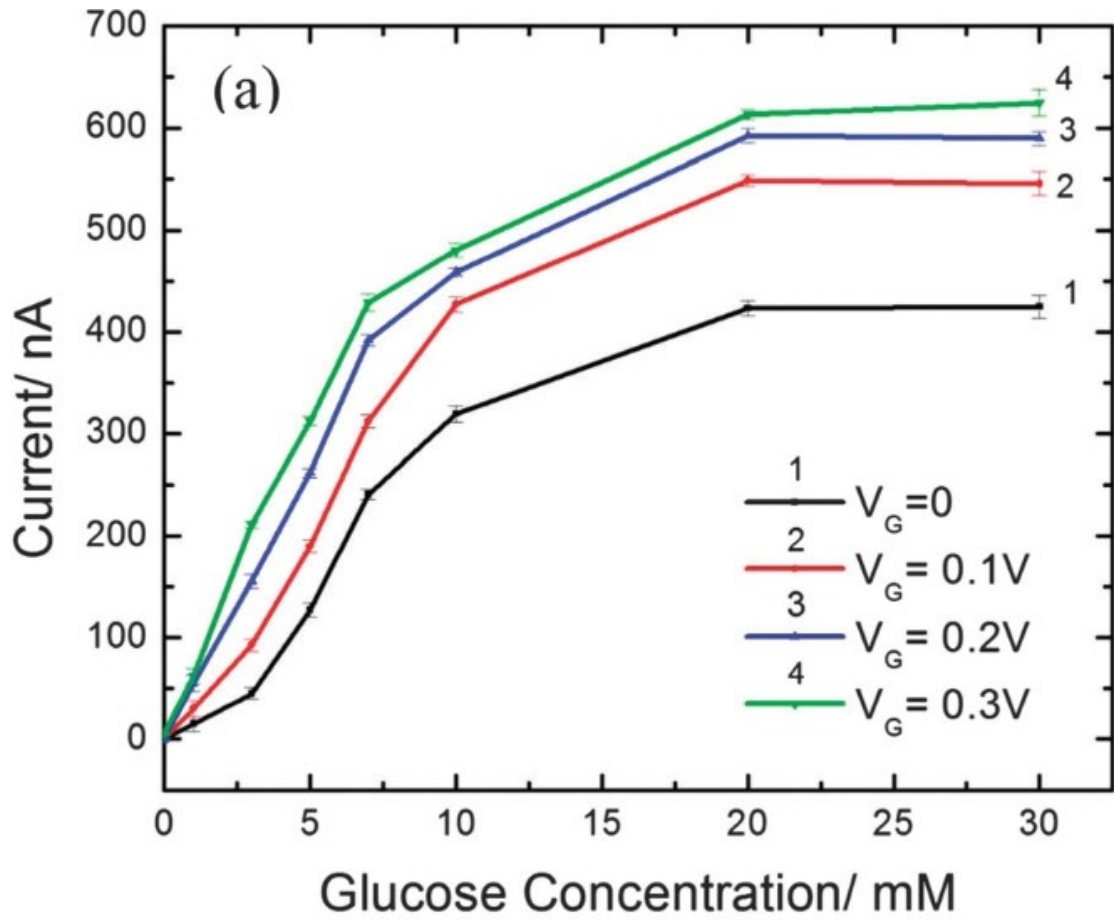


Fig 2-6  $V_G$ -dependent glucose calibration curves (Yau, Xu and Song, 2013). The current roughly changes as a linear response to the glucose concentrations.



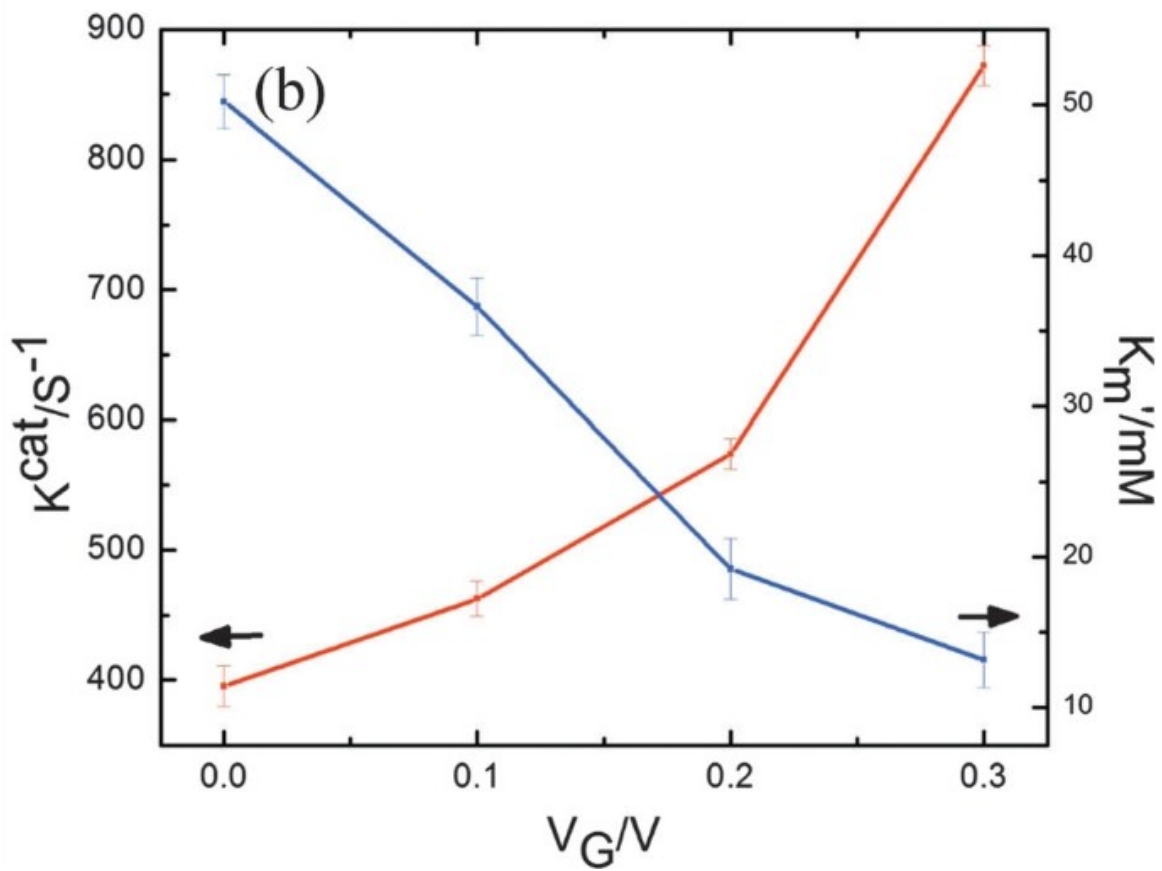


Fig 2-7 The  $V_G$ -dependent  $K_{cat}$  and  $K_m$  (Yau, Xu and Song, 2013)

# **CHAPTER III**

## **ELECTROSTATICALLY CONTROLLED METABOLISM OF GLUCOSE IN YEAST**

### **3.1 Summary**

Glucose metabolism process is one important part of cellular processes that convert glucose to energy for cell [1, 2]. The recent research on glucose metabolism focuses on its important role in the area of metabolic engineering and cell biology [3]. This work shows that the glucose consumption of yeast that was in contact with an electrode could be controlled using  $V_G$ . The observation that the glucose consumption qualitatively correlates to the production of the end products of glucose metabolism such as ethanol and ATP indicates that the entire process was glucose metabolism whose kinetics was controlled by applying  $V_G$  at an insulated gating electrode. In fact, experimental system used in this work is a transistor-like device, whose function is to control the glucose metabolism process using  $V_G$ . The results show a possible role for electrostatic means in several metabolism-related areas.

## 3.2 Materials and methods

### 3.2.1 Yeast preparation

Dried baker's yeast (*Saccharomyces cerevisiae*) purchased from Sigma Aldrich (YSC1) was cultivated for several hours at 30, in medium of deionized water, glucose and peptone.

### 3.2.2 System construction and operation

Pyrolysis graphite electrode (PG, GE Advanced coop) was used as the working electrode, which had an area of 1mm\*1mm, and is coated with mask. The yeast immobilized electrodes were prepared by depositing one drop (1mL) of yeast (Sigma Aldrich) onto the PG electrode surface and incubating under 27°C for 6 hours. And then the electrodes were washed with demonized water and dried at 27°C. A conventional three electrode cell was used in the Cyclic Voltammetry measurement (CH660C). An Ag/AgCl electrode was used as the reference electrode while platinum wire was used as counter electrode. The gating electrode, made by 0.5 mm diameter copper wire with an insulator thin, formed U-turn structure and was attached onto the surface of working electrode to suspend the yeast cells. PBS solution was prepared using deionizer water and diluted with  $\text{KH}_2\text{PO}_4$  and  $\text{Na}_2\text{HPO}_4$  until PH=6.8. The scan rate of the Cyclic Voltammetry system was set as 25mV/s and every data point was obtained by at least five duplication experiments. All the experiments were performed at 27°C.

### 3.2.3 Glucose, ATP and Ethanol Analyses

The anaerobic condition was achieved by purging solution with dry  $\text{N}_2$  for 1 hour. Samples of glucose in PBS were processed by the system in Fig 3-1 at room temperature using yeast immobilized electrodes at  $V_{\text{cell}} = 0.6\text{V}$  vs. Ag/AgCl for 1200s. Glucose

concentration was measured every 300s using commercial glucose meter, whose measuring range is 20-650mg/dl. Each time 5mL of solution was taken out to be measured. The meter was calibrated before use.

In aerobic glucose metabolism, glucose will be oxidized by glycolysis, Krebs cycle and electron transport chain in the presence of oxygen [4]. Adenosine triphosphate (ATP), one kind of end products in metabolic process, will be synthesized during metabolism process. Luminescence assay of ATP in yeast cell suspended in glucose sample, which were electrochemically processed in Fig 3-1, was used to reveal the ATP produced as function of  $V_G$ . The assay of ATP was performed using the BacTiter-Glo Microbial cell viability Assay kit. The luminescence was detected using Victor3 Multilabel Plate Counter and displayed as relative light units (RLU). The higher the luminescence intensity, the higher the concentration of ATP.

Ebulliometry of electrochemically processed glucose sample was performed to monitor the generation of ethanol. The ethanol concentration of sample was measured using an ebulliometer at room temperature. The production of ethanol was tested in a beaker containing 30mL of glucose solution. A 10mmx10mm carbon cloth was used as the working electrode. 100mM glucose solution was processed by the system in Fig3-1 at 27°C with and without  $V_G$  3 hours under anaerobic condition.

#### **3.2.4 Cyclic Voltammetry test**

Cyclic voltammetry (CH Instruments 660C) was carried out using the system shown in Fig 3-1 to characterize yeast induced oxidation of glucose [4]. The electrochemical test system was consisting with the three electrodes system with a volume of 2mL and CH660C workstation. The scan rate was set as 25mV/s and the

potentials were set from -400mV to 800 mV. To accurate the result, every experiments have been reproduced at least five times. Peaks were observed nearly the point of 200 mV.

### **3.2.5 Scanning electron microscopy**

A field emission scanning electron microscope, Hitachi FM-SEM 5000, was used to resolve the image of the immobilized yeast on electrode.

### **3.2.6 Nature electrostatic experiments**

To gain more evidence for the natural electrostatic field effect on the glucose metabolism processes, the anaerobic glucose metabolism experiments were performed using two electrodes system, which consisted of yeast immobilized carbon cloth electrode connected with insulator-coating electrode. The two electrodes were applied for providing electrostatic effect on the yeast cells. No current was observed between the two electrodes.

## **3.3 Results**

### **3.3.1 Electrochemistry of yeast immobilized electrode**

Fig3-2 shows the CVs obtained using yeast immobilized PG electrode with glucose solution under different conditions. None redox peaks can be recorded at bare electrode at potential from -0.4V to 0.8V. CV1 was obtained in the PBS solution whereas CV2 was obtained with glucose added to the PBS solution. CV1 only has one pair of weak redox peaks at the potential of 30mV vs. Ag/AgCl. These stable redox peaks were attributed to oxidation glucose of yeast. Previous work of CVs of yeast showed similar pattern of redox peaks [5]. The redox peaks indicate that it is possible to transfer electrons through

the yeast membrane directly [6]. Comparing CV2 to CV1, there is an increasing anodic current, indicating a possible oxidation process of glucose in yeast. The electron of glucose oxidation can migrate from cell to electrode. CV3 shows the further increase of anodic current and enhanced redox peaks caused by the applied positive  $V_G$ . These increases were attributed to the induced electric field between yeast cell and electrode resulting in the amplified anode current.

### **3.3.2 $V_G$ dependent of glucose depletion in yeast metabolism**

Glucose concentration changes with  $V_G$  under aerobic condition using yeast immobilized electrode (Fig3-3). Without applying  $V_G$ , a gradual decrease of glucose concentration is observed (Curve-1) with the increasing positive value of  $V_G$ , the glucose consumption rate will increase gradually at first and then will approach to a constant rate (Curve-2, -3, -4). It indicated that the effect of positive  $V_G$  can increase the glucose consumption result in faster decreasing in glucose concentration. Curve 5-7 proved that the glucose consumption rate will slower down with a negative  $V_G$ . A similar phenomenon is also observed in anaerobic condition (Fig 3-4). Compared the glucose depletion curves between aerobic and anaerobic condition, the anaerobic process has a faster consumption rate than those in aerobic process, consisting with its lower energy field [7]. In aerobic respiration, yeast can create more energy from one molecule glucose. Without oxygen, yeast will resort to fermentation that results in only producing 1/19 of energy in aerobic respiration [8].

The experimental measurements were conducted in the lag phase of yeast budding to avoid yeast reproduction. Before the electrochemical processing, a selected area of electrode was imaged by the scanning electron microscopy (SEM, Fig3-5). After 120 min

processing, the images kept the same. It eliminates the explanation that yeast growing causes the faster depletion of glucose.

### **3.3.3 $V_G$ dependent of ATP productions in metabolism**

The intensities of ATP luminescence assay under the aerobic condition are given by Fig 3-6. Within 60mins, the concentrations of ATP kept increasing under aerobic condition. With a higher  $V_G$ , the concentration of ATP was also higher. Since the ATP production is related to the glucose consumption (Fig 3-3), it can be conclude that the  $V_G$  is the reason for the increasing reaction rate of the glucose metabolism processes.

Under anaerobic condition, glucose metabolism process in yeast will go through fermentation pathway with ATP,  $CO_2$  and ethanol as the end products [17]. Fig 3-7, Fig 3-8 and Fig3-9 are the changes of ATP, ethanol and PH according to the different values of  $V_G$  under anaerobic condition.

The ATP production in glucose metabolism process and its changing trend under different  $V_G$  are given by Fig 3-7. Without applying the  $V_G$ , the ATP produced under anaerobic condition (Curve-1of Fig 3-7) is less than that under aerobic case (Curve-1of Fig 3-6). This difference consists with previous work, which proved that ATP produced in aerobic condition is 5 times per mole of glucose more than the ATP produced in anaerobic condition [9]. With the increasing positive value of  $V_G$ , the ATP production rate will increase gradually regardless of the anaerobic or aerobic condition (Fig 3-6, Fig 3-7). It indicates that the positive  $V_G$  can accelerate the glucose metabolism processes resulting in a faster productivity of ATP. On the contrast, a negative  $V_G$  will reduce the ATP productivity (curve-4, curve-5 of Fig 3-6).

The production efficiencies of ethanol increased gradually with the increasing

positive value of  $V_G$  (Fig 3-8), whereas the ATP productivity decelerated with a negative  $V_G$  (Fig 3-8).

As  $\text{CO}_2$  will be dissolved in the solution to form  $\text{H}_2\text{CO}_3$ , the presence of  $\text{CO}_2$  will change the PH of glucose solution [10]. The PH decreased from 5.9 to 5.3 as  $V_G$  increased from 0V to 1V (Fig 3-9) due to the increasing  $\text{CO}_2$  in the glucose metabolism process in solution.

The increasing amounts of productions induced by  $V_G$  could be elaborated by the yeast growing process. However, CVs tests and SEM described above clearly demonstrate that glucose was oxidized only by glucose metabolism process not by the cell growing. The ethanol concentration increasing at the batch test also indicated  $V_G$  could enhance the glucose metabolism process. We further examined whether has description of mechanism of  $V_G$  effect that would readily allow revealing realist.

#### **3.3.4 Nature electrostatic effect on the glucose metabolism**

The increases of the glucose consumption rate (Fig 3-11) and the ethanol production rate (Fig 3-12) are consisting with the increasing positive value of  $V_G$ . These patterns are similar to the ones in Fig 3-7 and Fig 3-8. The results prove that the natural electrostatic field could influence glucose metabolism.

### **3.4 Discussion**

The results have demonstrated that  $V_G$  can be used to control the kinetics of cellular glucose metabolic processes. The observation that the glucose consumption qualitatively correlates to the production of the end products of glucose metabolism such



as ethanol and ATP indicates that the entire process was glucose metabolism whose kinetics was controlled by  $V_G$ .

The relation between the  $V_G$  dependent glucose depletion and the  $V_G$  dependent production of end products reveals that glucose metabolism was controlled by  $V_G$ . The metabolic pathway is equivalent to the channel of field effect transistor (FET) whereas the glucose consumption and production of the end products are output quantities (Fig 3-10).

Previously, it has been demonstrated by previous works that applying an external voltage to a glucose oxidase (GOx) immobilized working electrode of a modified three-electrode electrochemical cell would result in an enhancement of glucose oxidation current. It was explained as the increased electron transfer between the active site of enzyme and the electrode as the result of the reducing height of electron tunnel barrier [11, 12, our work in chapter II]. The electron tunnel barrier is involving the electron transfer pathway between active center of enzyme and electrode [13]. Glucose metabolism in yeast involves redox reactions catalyst by different kind of redox enzymes. For instance, the reduction of the  $NAD^+$  to form NADH by glyceraldehyde-3-phosphate dehydrogenases in glycolysis, or by alcohol dehydrogenase for maintaining redox balance of cell, either or both processes being influenced by induced electric field [5]. The electron will travel from NADH to NADH dehydrogenase (NDI) who is located on the electron transport chain in yeast cell (Fig 3-13). The NDI is used to transport the electron from FAD activity center to ubiquinone (UBQ) [14]. The  $V_G$  will induce electric field, whose component is opposite to the electron's transfer movement through enzyme, controlling the effective height of barrier so that the electron transfer rate can be

increased or decreased [15]. Similar controlled electron transfer also happens in other redox enzymes involved in the glucose metabolism, leading to faster production of products. The positive  $V_G$  will totally reduce the height of electron tunnel barrier, while the negative  $V_G$  will increase the electron tunnel barrier to reduce the electron transfer rate. The observation will provide evidence for mechanism.

In the glucose metabolism process, glucose will be catalyzed to ethanol and  $H_2O$  by redox enzymes. The final production depends on the enzyme activity which is involved in the redox catalysis processes. The redox enzymes will absorb energy from the electric field induced by electrostatic effect to make transition of electron energy level on the surface of enzymes [16]. It will break the chemical bounds, resulting in instability of enzyme structure. Enzymes will expose more activity sites on the surface, resulting in increasing the surface area which involved the catalytic reaction, leading to an increasing activity of enzymes.

### 3.5 References

- [1] McKnight S L. On getting there from here[J]. Science(Washington), 2010, 330(6009): 1338-1339.
- [2] Mathews, C. K., van Holde, K. E., and Ahern, K. G., Biochemistry, 3rd edition ed. (Addison Wesley Longman, San Franscisco, 2000).
- [3] Ray L B. Metabolism is not boring[J]. Science, 2010, 330(6009): 1337-1337.

- [4] Fernie A R, Carrari F, Sweetlove L J. Respiratory metabolism: glycolysis, the TCA cycle and mitochondrial electron transport[J]. *Current opinion in plant biology*, 2004, 7(3): 254-261.
- [5] Rawson F J, Gross A J, Garrett D J, et al. Mediated electrochemical detection of electron transfer from the outer surface of the cell wall of *Saccharomyces cerevisiae*[J]. *Electrochemistry Communications*, 2012, 15(1): 85-87.
- [6] Shukla A K, Suresh P, Berchmans S, et al. Biological fuel cells and their applications[J]. *Current Science*, 2004, 87(4): 455-468.
- [7] Rodrigues, F., Ludovico, P., and Leao, C., in *Biodiversity and Ecophysiology of Yeasts* edited by G. Péter and C. Rosa (Springer Berlin Heidelberg, 2006), Vol. The Yeast Handbook 2006, pp. 101.
- [8] Sherman F. The effects of elevated temperatures on yeast. II. Induction of respiratory - deficient mutants[J]. *Journal of cellular and comparative physiology*, 1959, 54(1): 37-52.
- [9] Lagunas R. Misconceptions about the energy metabolism of *Saccharomyces cerevisiae*[J]. *Yeast*, 1986, 2(4): 221-228.
- [10] Loerting T, Bernard J. Aqueous carbonic acid (H<sub>2</sub>CO<sub>3</sub>)[J]. *ChemPhysChem*, 2010, 11(11): 2305-2309.
- [11] Choi Y, Yau S T. Field-Effect Enzymatic Amplifying Detector with Picomolar Detection Limit[J]. *Analytical chemistry*, 2009, 81(16): 7123-7126.
- [12] Choi Y, Yau S T. Field-controlled electron transfer and reaction kinetics of the biological catalytic system of microperoxidase-11 and hydrogen peroxide[J]. *AIP Advances*, 2011, 1(4): 042175.
- [13] Tans S J, Verschueren A R M, Dekker C. Room-temperature transistor based on a single carbon nanotube[J]. *Nature*, 1998, 393(6680): 49-52.
- [14] VRIES S, GRIVELL L A. Purification and characterization of a rotenone - insensitive NADH: Q6 oxidoreductase from mitochondria of *Saccharomyces cerevisiae*[J]. *European journal of biochemistry*, 1988, 176(2): 377-384.
- [15] Westerhoff H V, Tsong T Y, Chock P B, et al. How enzymes can capture and transmit free energy from an oscillating electric field[J]. *Proceedings of the National Academy of Sciences*, 1986, 83(13): 4734-4738.
- [16] Westerhoff H V, Tsong T Y, Chock P B, et al. How enzymes can capture and transmit free energy from an oscillating electric field[J]. *Proceedings of the National Academy of Sciences*, 1986, 83(13): 4734-4738.
- [17] Sainz J, Pizarro F, Pérez - Correa J R, et al. Modeling of yeast metabolism and process dynamics in batch fermentation[J]. *Biotechnology and Bioengineering*, 2003, 81(7): 818-828.

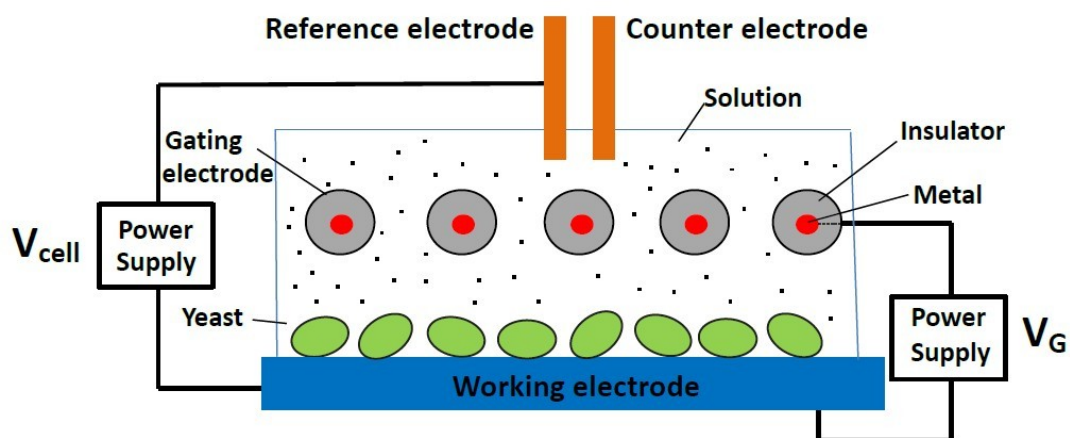


Fig 3-1 Electrostatically controlled system

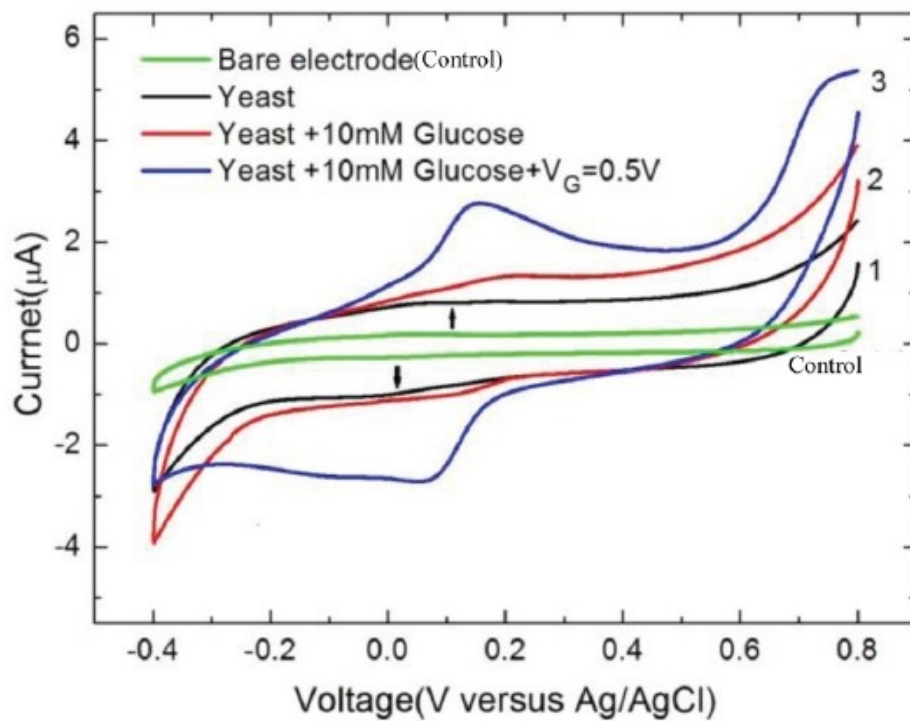


Fig 3-2 CVs showing the yeast-induced oxidation of glucose.

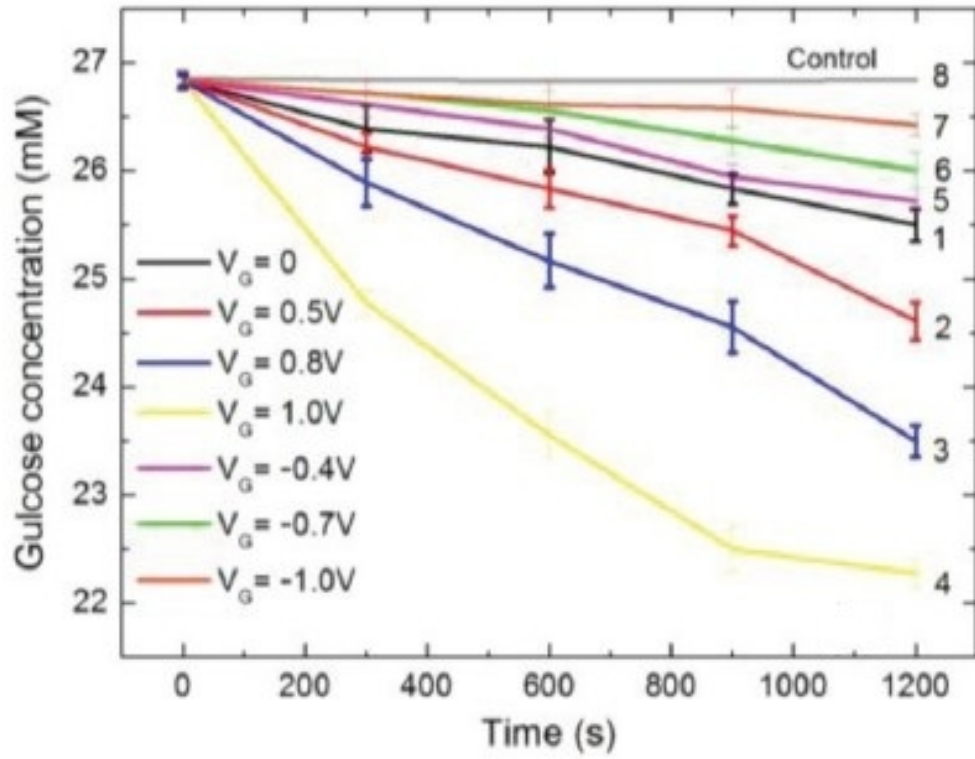


Fig 3-3  $V_G$  effect on glucose consumption in the aerobic condition

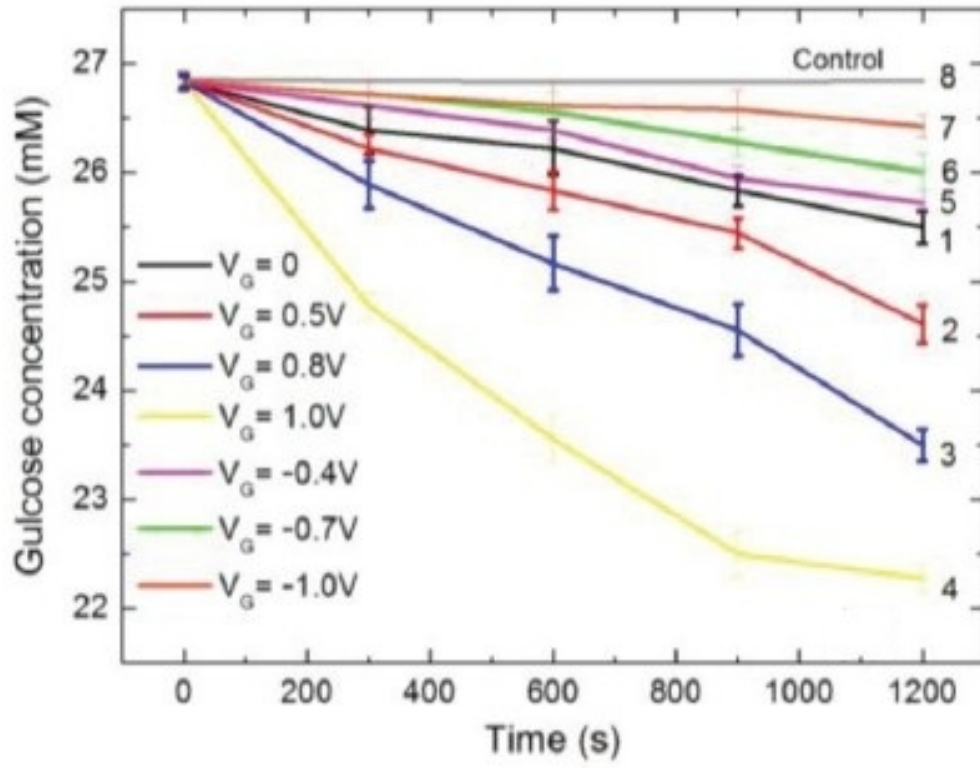


Fig 3-4  $V_G$  effect on glucose consumption in the anaerobic condition

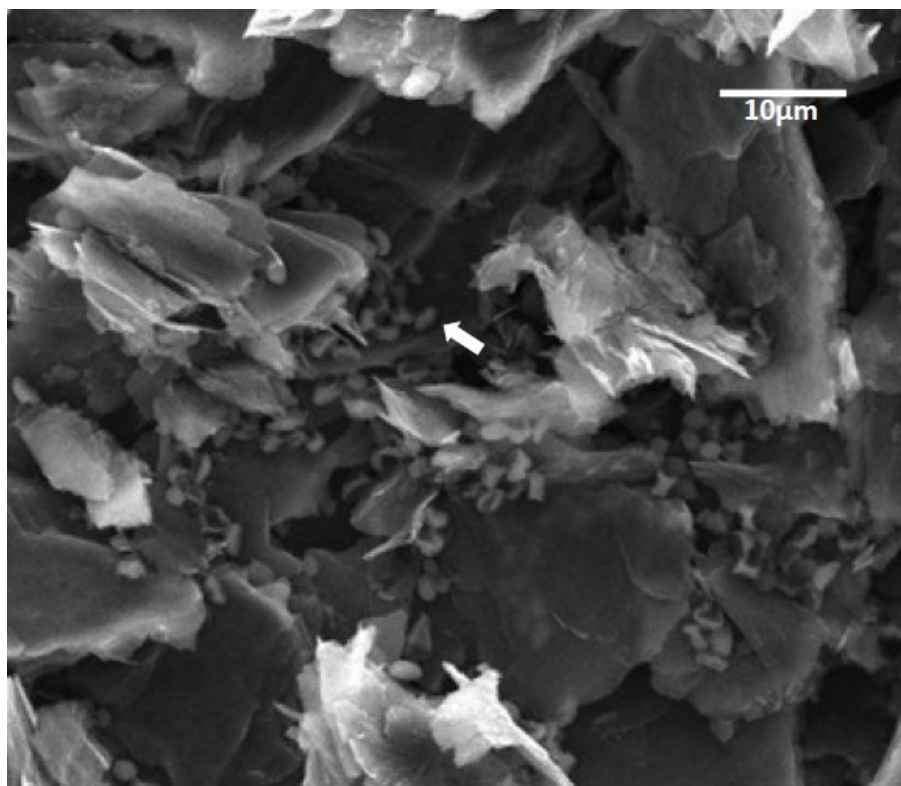


Fig 3-5 SEM image of yeast-immobilized electrode before electrochemical processing

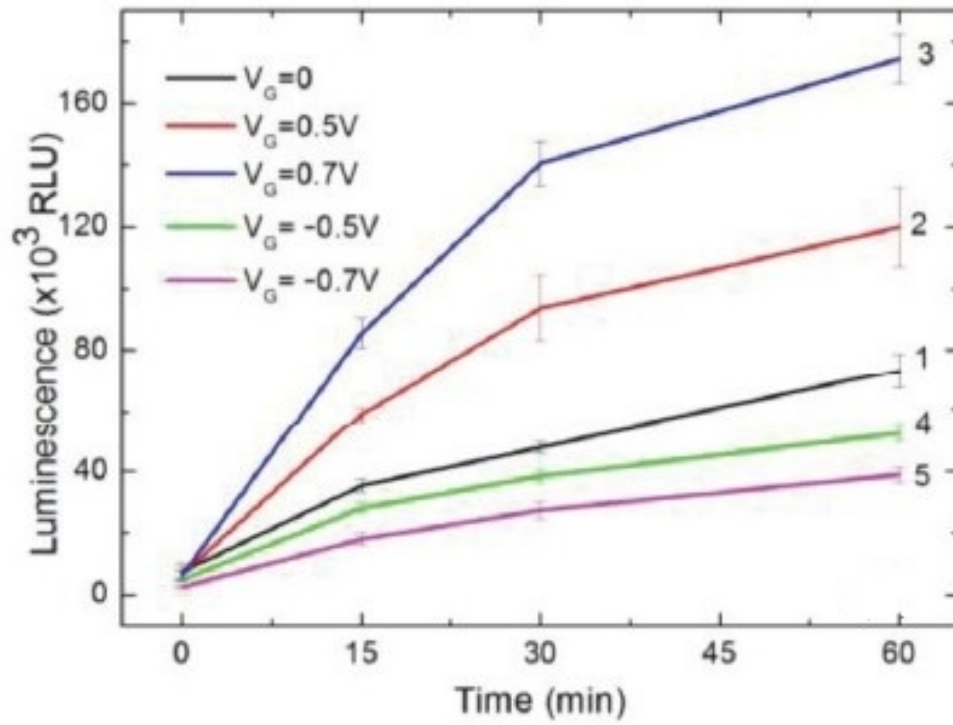


Fig 3-6  $V_g$ -controlled production of ATP under the aerobic condition



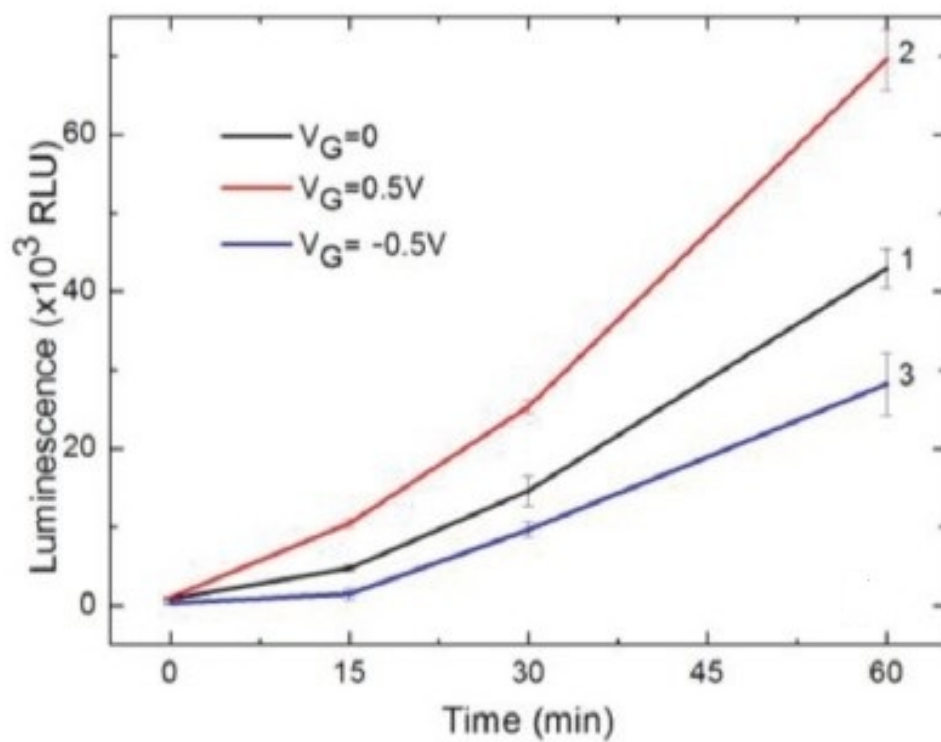


Fig 3-7 the  $V_G$ -controlled production of ATP under the anaerobic condition. Curve-1: the gradual increasing in amount of ATP at  $V_G=0V$ . Curve-2: the gradual increasing in amount of ATP at  $V_G=0.5V$ . Curve-3: the gradual increasing in amount of ATP at  $V_G=-0.5V$ .

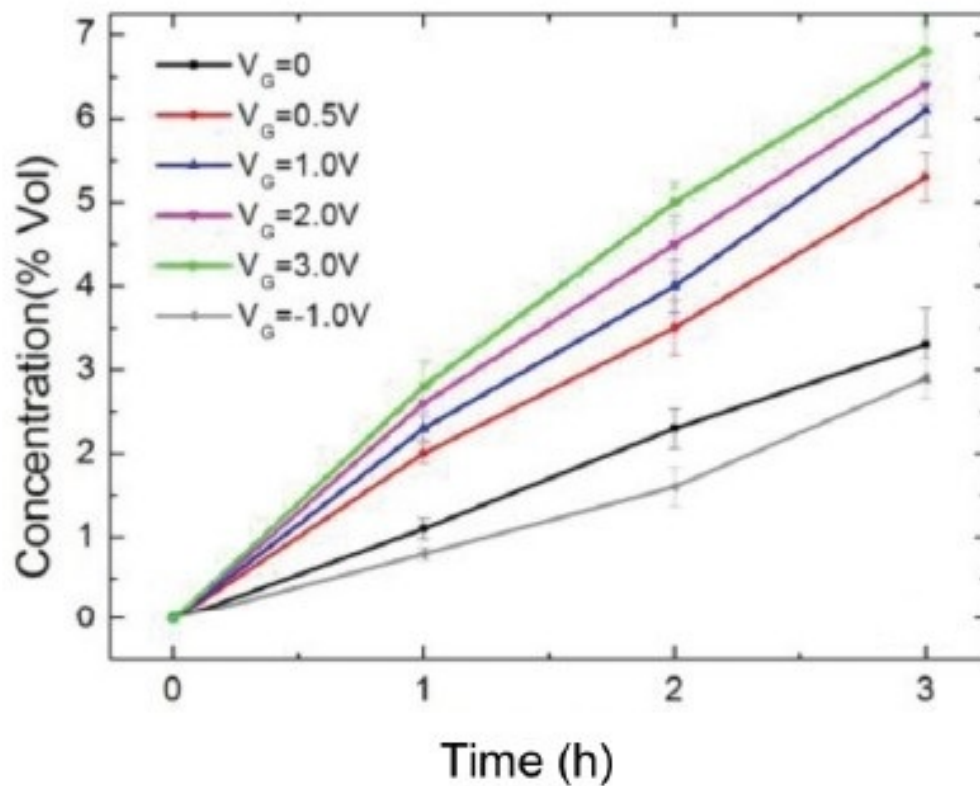


Fig 3-8 the  $V_G$ -controlled generation of ethanol. The produced ethanol corresponding to different values of  $V_G$  under anaerobic condition using yeast immobilized electrode during 3 hours.

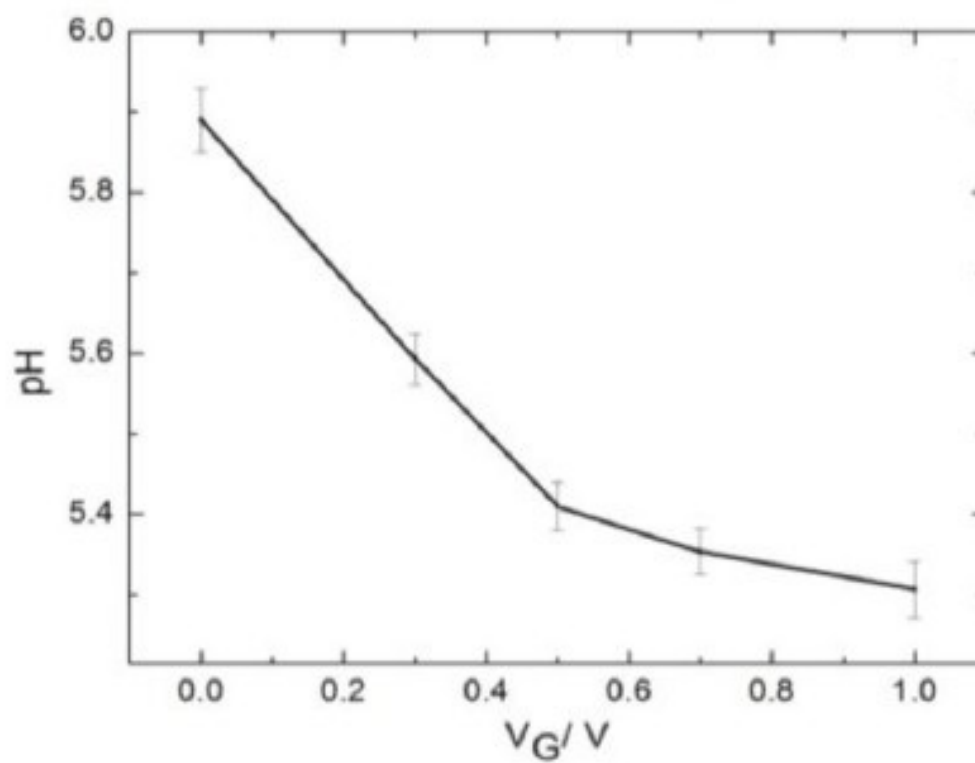


Fig 3-9 the change in pH under the anaerobic condition. PH changing of electrochemically processed glucose solution as a result of  $V_G/V$  within 1 hour.

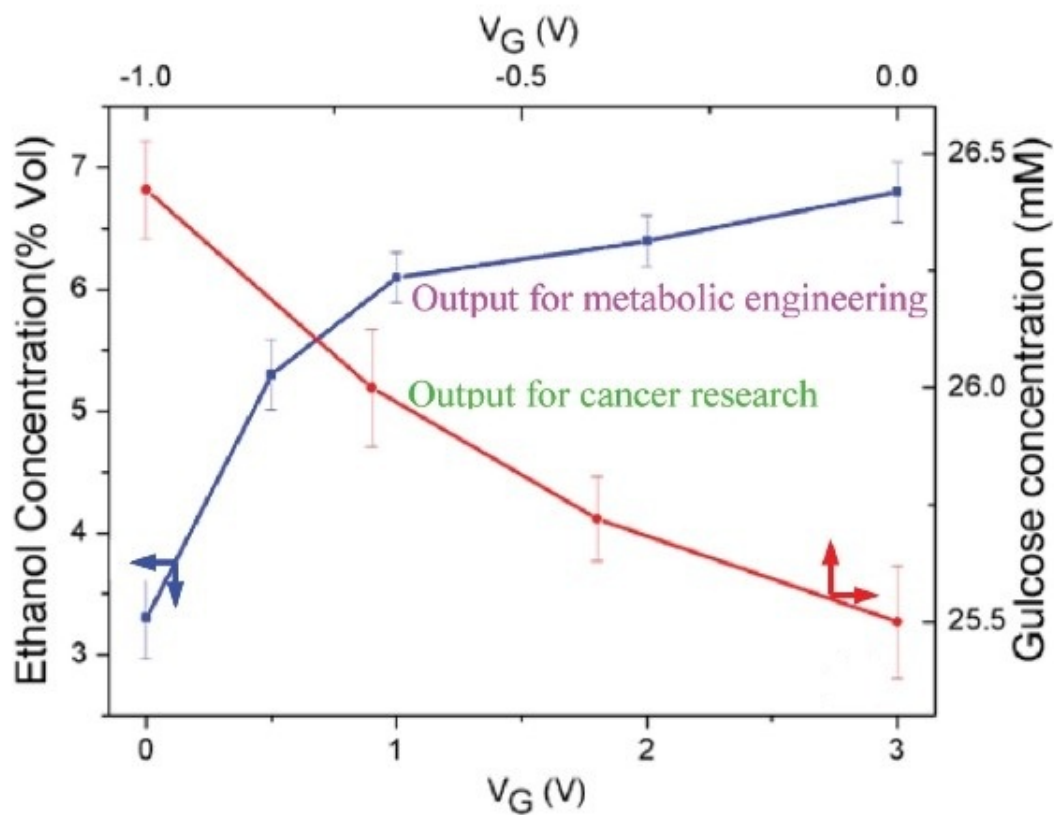


Fig 3-10 Transfer characteristics of the metabolic transistor. The field effect transistor (FET) with  $V_G$  being used to control the output quantity. The characteristics of metabolic transistor which has glucose output is derived from the value at 1200s of Curve1 5-7 in Fig 3-3 and output from the value at 3h of positive  $V_G$  value in the Fig 3-9.

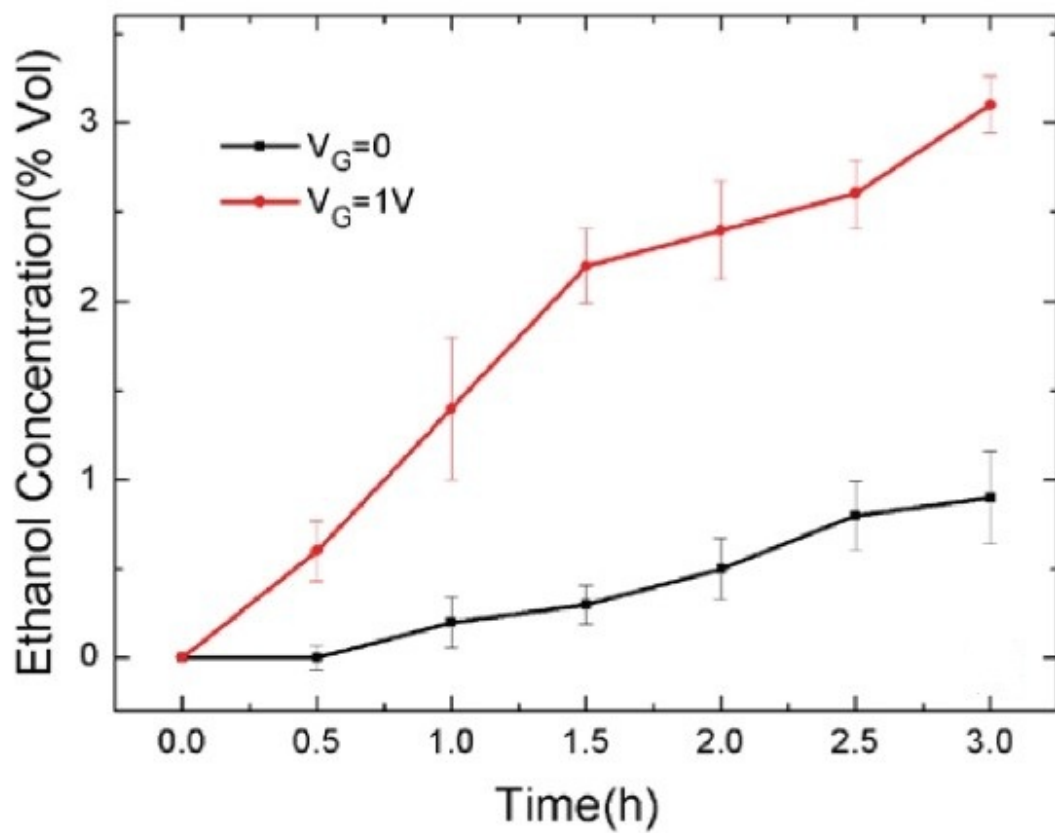


Fig 3-11 The ethanol production using the two-electrode system without current in the entire process

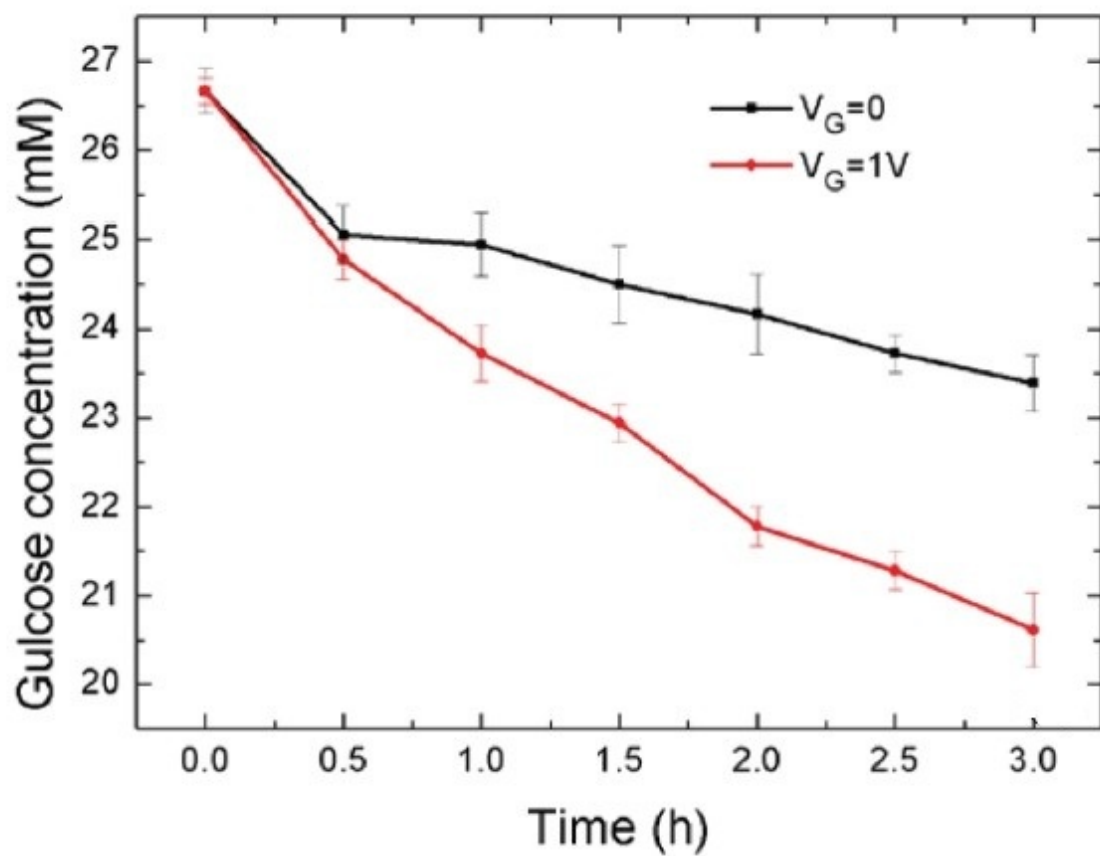


Fig 3-12 the glucose consumption in the two-electrode system without current in the entire process

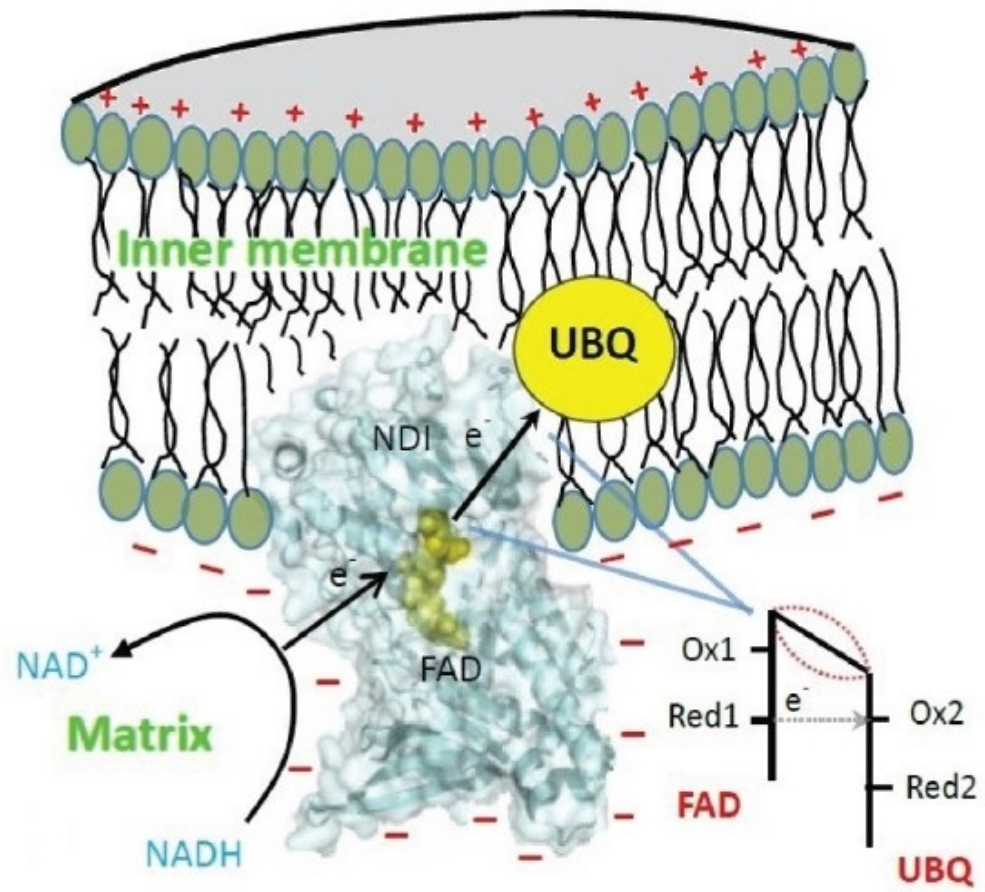


Fig 3-13 Scenario for electron shuttle through enzymes

## **CHAPTER IV**

### **THE ELECTROSTATICALLY ENHANCED PERFORMANCE OF MICROBIAL FUEL CELL**

#### **4.1 Summary**

This work shows that electric fields can control power output of the microbial fuel cells (MFCs) -by improving fuel cell efficiency and power density. The yeast was used as the catalyst of the MFCs anodes. After applying a voltage of 0.5V to the anode of a compact two-chamber microbial fuel cell, we observed an increase of the open circuit voltage (OCV) of cell with the range from 0.30V to 0.47V. The gating voltage ( $V_G$ ) also extended the operation current and increased power output. The improved performance could not show that any of the extra energy spent on the microbial fuel cell. The coulombic efficiencies (CEs) -were increased from 6% to 15% by applying gating voltage, which suggested that the gating voltage can improve the performance by promoting electron shuttle between microorganism and anode. The power density was significantly higher than those values obtained for the normal experiments. Because the gating voltage lowered electron tunnel barriers resulting in the enhancing electron transfer in anode compartment, which led to improvements of the performance of



MFCs.

## 4.2 Materials and methods

### 4.2.1 MFC construction and operation

A type of double-chambers MFCs was operated to use in this work: two-chambers cube MFC (C-MFC) (Fig 4-1). This MFC has two glass chambers with a length of 5cm. The liquid volumes of two chambers are all 100 ml, separated by proton exchange membrane (PEM). The carbon cloth (non-wet proofed, Tp1-120, Toray, Inc.) was used to the anode and cathode with a J-cloth of 10 cm<sup>2</sup> for separating. PEM was clipped on the center site between anode chamber and cathode chamber, and sealed with a rubber ring on each side. Current density was calculated based on the area of the PEM. Make sure that the distance between anode electrode and cathode electrode is less than 2cm. The lesser distance between two electrodes can reduce internal resistance and increase power output [1, 17]. A reference electrode (Ag/AgCl) was located in anode chamber. All reactor chambers were tested in room temperature. A voltage source  $V_G$  was applied between the anode and an additional gating electrode, which was formed by bending an insulator-coated copper wire.

### 4.2.2 Membranes

Nafion<sup>TM</sup> 117 (DuPont Co., Delaware) was washed in H<sub>2</sub>O<sub>2</sub> (30% v/v) and deionized water. Then wash with PBS solution. The PEM should be reserved in the water or PBS solution before tests. Each membrane was soaked by PBS solution before all tests to make sure expansion of PEM.

### 4.2.3 Operation of MFC

*Saccharomyces cerevisiae* (YSC1, Sigma Aldrich) or baker yeast was used as biocatalyst for anode. Dried yeast was cultured for 20 hours at 30°C in the medium containing glucose, peptone, 160mM fructose, PH=7. A volume of 80ml of cultured medium was mixed with 120 mM glucose by using PBS, then adjusted to PH=7.0 and used as the anolyte. Methylene blue at 50mM was added to the anolyte as the mediator. The catholyte was 80mL of PBS with 50mM of Potassium ferrocyanide as the mediator. Initially, the anolyte was purged with dry nitrogen for 60 min. Then, the anode potential and OCV was measured versus Ag/AgCl reference electrode. And cathode potential was deduced from the OCV and anode potential.

### 4.2.4 Monitoring voltage and power

The MFC was linked with the external changing resistor (200M  $\Omega$ ) in the circuit. The voltage (V) should be continuously recorded using digital multimeter (Keithley Instruments 2000, OH) connected to computer while changing the resistor. Current (I), power ( $P=IV$ ) and coulombic efficiency (CE) were calculated from the equation [10]. The power density of MFC was calculated by power value divided PEM area. The internal resistance of MFC was measured from the slop of plots of V and I by using  $V=E_{\text{cell}} - IR_{\text{int}}$ , where  $E_{\text{cell}}$  is the external voltage of the cell.

### 4.2.5 Electrochemistry measurement

Cyclic voltammetry (CH Instruments 660C) was carried out to test reaction happened on the yeast biofilm. The electrochemical test system was consisting with the three electrodes system and CH660C workstation. The Ag/AgCl electrode was used to the reference electrode and platinum wire was used to counter electrode. The scan rate of

25mV/s and the potentials were from -400 to 800 mV had been recorded in the experiments and every detection experiments must be processed for at least five times to reach the similar result to obtain. Peaks were obtained in the range of 0 to 200 mV.

#### **4.2.6 Determination of Fuel cell efficiency**

The microbial fuel cell efficiency is determined by reaction happened in anode. The efficiency of glucose metabolism reaction could be shown:  $\text{Efficiency} = G/H$ , where H is enthalpy of glucose, G is Gibbs free energy [2]. And coulombic efficiency was calculated as  $E = (C_p/C_t) \times 100\%$ , where  $C_p$  is total coulombs by the current over time, and  $C_t$  is the theoretical amount of coulombs that products from glucose [3].

### **4.3 Results**

#### **4.3.1 Cyclic voltammetry of yeast microbial fuel cell**

Under the anaerobic condition, yeast would go through alcohol fermentation process during which glucose will be oxidized to alcohol by alcohol dehydrogenase [4]. The redox current is coming from NADH which is produced in fermentation process [5]. The experiments of the cyclic voltammetry of yeast were carried out with the system showing in the Fig4-1 to study the effect of gating voltage. The cyclic voltammetry was obtained using yeast immobilized PG electrode in glucose solution under different condition (Fig4-2). CV1 was obtained in PBS and CV2 was obtained with glucose added to PBS solution. CV1 and CV2 have shown a pair of weak redox peaks at 100mV vs. Ag/AgCl (Fig4-2). This phenomenon indicates that there are redox enzymes in cell membrane serving as electron shuttles in redox process. In mediated electron transfer in fuel cell need redox mediator as electron shuttles to help electron transfer to electrode

[6]. Methylene blue (MB), as one kind of lipophilic electron transfer shuttles, is able to go through the yeast membrane along with electrons [7]. One pair of peak in CV3 (Fig4-2) is due to adding mediator, MB, to the anolyte. MB can interact with electron transport chain and capture the electrons from the reaction degraded pyruvate resulting in increasing redox peaks. When the  $V_G=0.5V$  and  $V_G=0.7V$  are applied, the progressively enhanced redox peaks were acquired (CV4, CV5, Fig4-2) respecting to electrostatically enhanced redox process. Therefore, the  $V_G$  can cause an increase in the mediated anodic current.

#### **4.3.2 Open circuit voltage changing in the presence of electrostatic effect**

The  $NAD^+/NADH$  redox couple will determine the potential of anode if there is no mediator in anode, even if oxidation process of NADH is very slow. With the present of MB in anode, the potential of anode will be determined by the redox reaction of MB [8]. From Fig4-3, we can notice that cathode potential was always 0.57V regardless of gating voltage. When mediator is present in cathode, the potential of cathode is determined by the redox reaction of  $PF_{(oxidized)} / PF_{(reduced)}$ ; and therefore the potential of cathode keep positive [9]. With  $V_G=0V$ , the anode potential was measured to be 0.27V; under the condition of  $V_G=0.5V$ , the anode potential was measured to be 0.1V (Fig4-3). The anode potential lowed with the increase of gating voltage, which indicates that the anode oxidation reaction was dominated by gating voltage. OCV was increasing at the same time (Fig4-3). It indicates that the electrostatical effect can significantly enhance the electron transfer from NADH to mediator leading to the drop of the anode potential.

#### **4.3.3 Fuel cell behavior under loading**

The carbon cloth electrode was exposed in the solution with a great number of

surface areas. Small electrode size will lower the power output in MFCs due to limited proton conductivity [10]. For researching on the performance of microbial fuel cell under different loading, the fuel cell was operated by connecting to an external changing resistor and different potential changing across the resistor would be recorded. For each test, the fuel cell was running with external resistance for at least 15 min. As the result, when the resistance was more than 1K ohms, the potential has decreased significantly (Fig4-4). And it has also been observed that the current increased with the decreasing load because of the increasing intern resistant losses. Fig 4-4 shows the polarization curve (voltage VS current) and the power curve (power VS current) of MFC at different  $V_G$  condition. The applying of  $V_G=0.5V$  appears to extend the maximum current density of MFC from  $9.5mA/m^2$  to  $22mA/m^2$ . Both polarization curves show that the activation loss is presumable due to the use of mediator. The polarization curves show that the extended operation current is accompanied by a reduced concentration loss.  $V_G$  caused the peak power density shifted from  $6.5mA/m^2$  to  $14mA/m^2$  and boosted the maximum of peak power from  $145mW/m^3$  to  $200mW/m^3$ . The internal impedance is an important factor for determining performance of MFC. The polarization curves also show that  $V_G$  appears to reduce the Ohmic loss.

#### **4.3.4 Fuel cell efficiency**

Coulombic efficiency (CE) was also investigated at different loadings. Fig4-5 shows the calculated CEs of the MFCs using cell current. Clearly, under the condition of  $V_G=0.5V$ , the MFC had the highest CE. The applying of  $V_G=0.5V$  appears to improve the Coulombic efficiency of MFC from 6% to 15%. It is also observed that the Coulombic efficiency of the MFCs tended to increase as the current density increasing

due to the decrease of the resistance. It indicates that the current flow affects the Coulombic efficiency. Since the Coulombic efficiency indicates the actual amount of coulombs transferring from substrate to anode, the improved performance of MFCs also suggests that there could be more electron transfer between mediator and electrode [10].

#### 4.4 Discussion

In yeast microbial fuel cell, glucose oxidation reaction provides energy [11]. The potential of anode and cathode were depended on every redox reaction happening on their chambers. The potential of cathode is determined by the redox reaction of  $\text{PF}_{(\text{oxidized})} / \text{PF}_{(\text{reduced})}$  [9]. Also, the redox of glucose will determine the potential of anode. However the energy generation is hardly to be extracted from yeast cell due to the difficulties of electron transfer processes through yeast cell membrane [5]. On the contrast, mediator can pass through cell membrane easily and carry great number of electrons. These features provide the promising future that mediator can be used as the electrochemical shuttle to make electrons from metabolic biocatalyst [12].

It has been demonstrated by previous works that applying an external voltage to a glucose oxidase (GOx) immobilized working electrode of a modified three-electrode electrochemical cell would result in an enhancement of glucose oxidation current [18]. It was explained as the increased electron transfer between the active site of GOx and the electrode as the result of the reducing height of electron tunnel barrier [13]. Many redox reactions catalyzed by different kind of redox enzymes were involved in yeast Glucose metabolism. For instance, the reduction of the  $\text{NAD}^+$  to form NADH by glyceraldehyde-3-phosphate dehydrogenases in glycolysis, or by alcohol dehydrogenase for maintaining

redox balance of cell, either or both processes being influenced by induced electric field [15]. The enhanced electron transfer was due to the induced electric field, contributing to a rapid recycling of the  $\text{NAD}^+/\text{NADH}$  redox couple because of the participation of enzyme. Mediators interact with electron transport chain and make electron from tricarboxylic acid cycle degradation of pyruvate via the trans-plasma membrane electron transfer (tPMET) [16]. The induced field could lower the tunnel barrier of the electron transfer process from NADH to mediator, and could also facilitate oxidation process of mediator at the electrode; therefore it could enhance the efficiency of the final step of transfer electron from yeast cell. This result is evidenced by the lower anode potential and by extended MFC operation from  $9.5\text{mA/m}^2$  to  $22\text{mA/m}^2$  with the enhanced coulombic efficiency.

Concentration losses will happen when transport rate of species from the acceptor is limited by the current output. Biomass production was estimated based on anaerobic respiration and maintenance energy, but direct measurements are needed in future studies to improve substrate mass balances. Some concentration losses are also possible due to production or electron accepters. The fast recycling of  $\text{NAD}^+/\text{NADH}$  couple and the enhanced electron transfer from NADH to the mediator may cause more reducing mediator available to the electrode and therefore will decrease the concentration loss. The reduced concentration loss resulting from decreasing the ratio between the oxidized of  $V_G$  and the reducing species at the anode would lead to a drop in the anode potential. When applying  $V_G$ , coulombic efficiency is increased because of the enhanced electron transfer from microbe to anode.

Enhancing electron transfer process from microbe to the anode is essential to

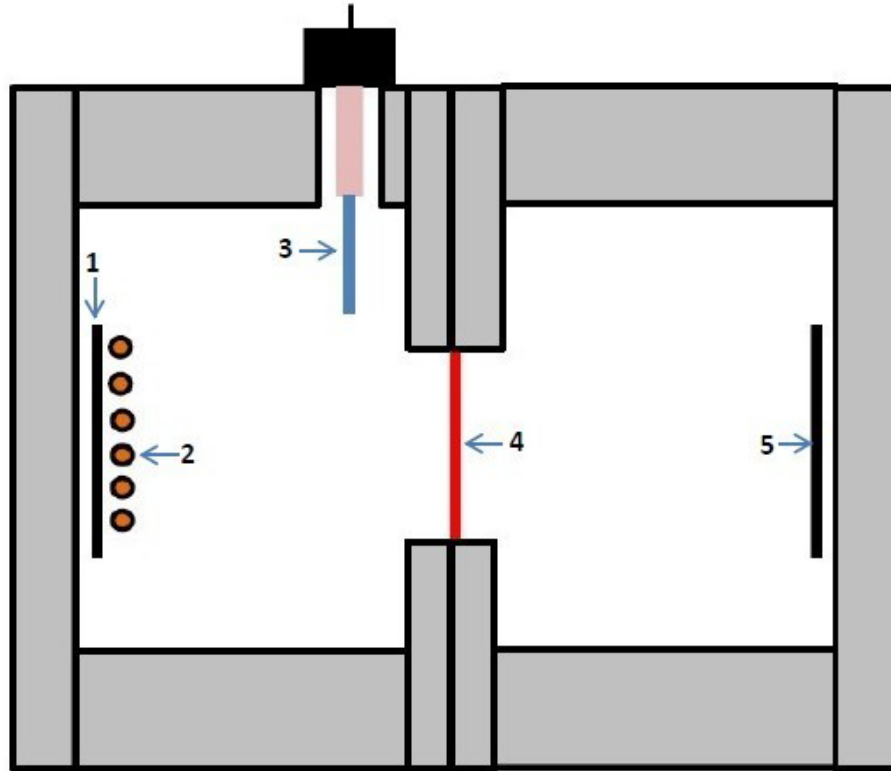
improve the performance of MFC. Different methods including direct transfer and the use of mediator have been applied to enhance electron transfer. The electrostatically effect enhanced performance of MFC was achieved without spending any energy on MFC since no current was measure in the additional anode circuit. Therefore, the electrostatically effect can be used as a promising method to improve the output.

#### 4.5 References

- [1] Logan B E, Hamelers B, Rozendal R, et al. Microbial fuel cells: methodology and technology[J]. *Environmental science & technology*, 2006, 40(17): 5181-5192.
- [2] Kim J R, Min B, Logan B E. Evaluation of procedures to acclimate a microbial fuel cell for electricity production[J]. *Applied microbiology and biotechnology*, 2005, 68(1): 23-30.
- [3] Liu H, Cheng S, Logan B E. Power generation in fed-batch microbial fuel cells as a function of ionic strength, temperature, and reactor configuration[J]. *Environmental science & technology*, 2005, 39(14): 5488-5493.
- [4] Wang Z, Zhuge J, Fang H, et al. Glycerol production by microbial fermentation: a review[J]. *Biotechnology Advances*, 2001, 19(3): 201-223.



- [5] Shukla A K, Suresh P, Berchmans S, et al. Biological fuel cells and their applications[J]. *Current Science*, 2004, 87(4): 455-468.
- [6] Schaetzle O, Barrière F, Baronian K. Bacteria and yeasts as catalysts in microbial fuel cells: electron transfer from micro-organisms to electrodes for green electricity[J]. *Energy & Environmental Science*, 2008, 1(6): 607-620.
- [7] Wilkinson S, Klar J, Applegarth S. Optimizing biofuel cell performance using a targeted mixed mediator combination[J]. *Electroanalysis*, 2006, 18(19 - 20): 2001-2007.
- [8] Lee S K, Mills A. Novel photochemistry of leuco-Methylene Blue[J]. *Chemical Communications*, 2003 (18): 2366-2367.
- [9] Nørskov J K, Rossmeisl J, Logadottir A, et al. Origin of the overpotential for oxygen reduction at a fuel-cell cathode[J]. *The Journal of Physical Chemistry B*, 2004, 108(46): 17886-17892.
- [10] Oh S E, Logan B E. Proton exchange membrane and electrode surface areas as factors that affect power generation in microbial fuel cells[J]. *Applied microbiology and biotechnology*, 2006, 70(2): 162-169.
- [11] Chaudhuri S K, Lovley D R. Electricity generation by direct oxidation of glucose in mediatorless microbial fuel cells[J]. *Nature biotechnology*, 2003, 21(10): 1229-1232.
- [12] Zhao J, Wang M, Yang Z, et al. The different behaviors of three oxidative mediators in probing the redox activities of the yeast *Saccharomyces cerevisiae*[J]. *Analytica chimica acta*, 2007, 597(1): 67-74.
- [13] Tans S J, Verschueren A R M, Dekker C. Room-temperature transistor based on a single carbon nanotube[J]. *Nature*, 1998, 393(6680): 49-52.
- [14] Cho S H, Collet J F. Many roles of the bacterial envelope reducing pathways[J]. *Antioxidants & redox signaling*, 2013, 18(13): 1690-1698.
- [15] Bakker B M, Overkamp K M, Maris A J A, et al. Stoichiometry and compartmentation of NADH metabolism in *Saccharomyces cerevisiae*[J]. *FEMS microbiology reviews*, 2001, 25(1): 15-37.
- [16] Medina M Á, Castillo - Olivares A D, De Castro I N Ñ. Multifunctional plasma membrane redox systems[J]. *Bioessays*, 1997, 19(11): 977-98
- [17] Oh S E, Logan B E. Proton exchange membrane and electrode surface areas as factors that affect power generation in microbial fuel cells[J]. *Applied microbiology and biotechnology*, 2006, 70(2): 162-16
- [18] Choi Y, Yau S T. Ultrasensitive biosensing on the zepto-molar level[J]. *Biosensors and Bioelectronics*, 2011, 26(7): 3386-3390.



- 1 Anode                      2 Additional electrode  
 3 Reference electrode    4 Proton exchange membrane  
 5 Cathode

Fig 4-1 Schematic description of additional electrode-anode system

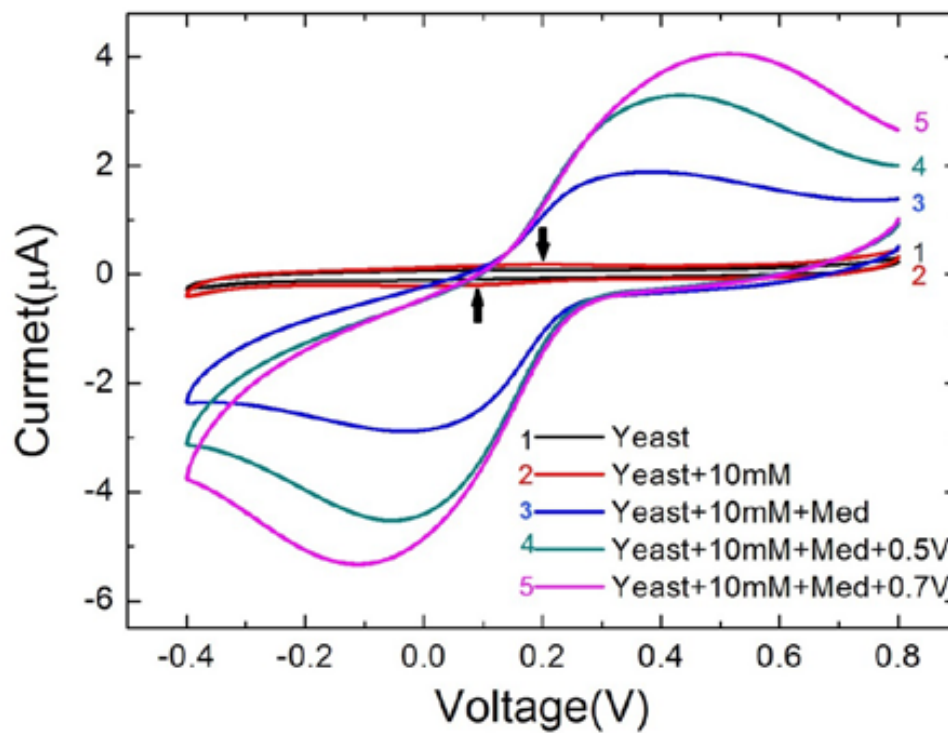


Fig 4-2 CVs of yeast-immobilized electrode under different conditions.

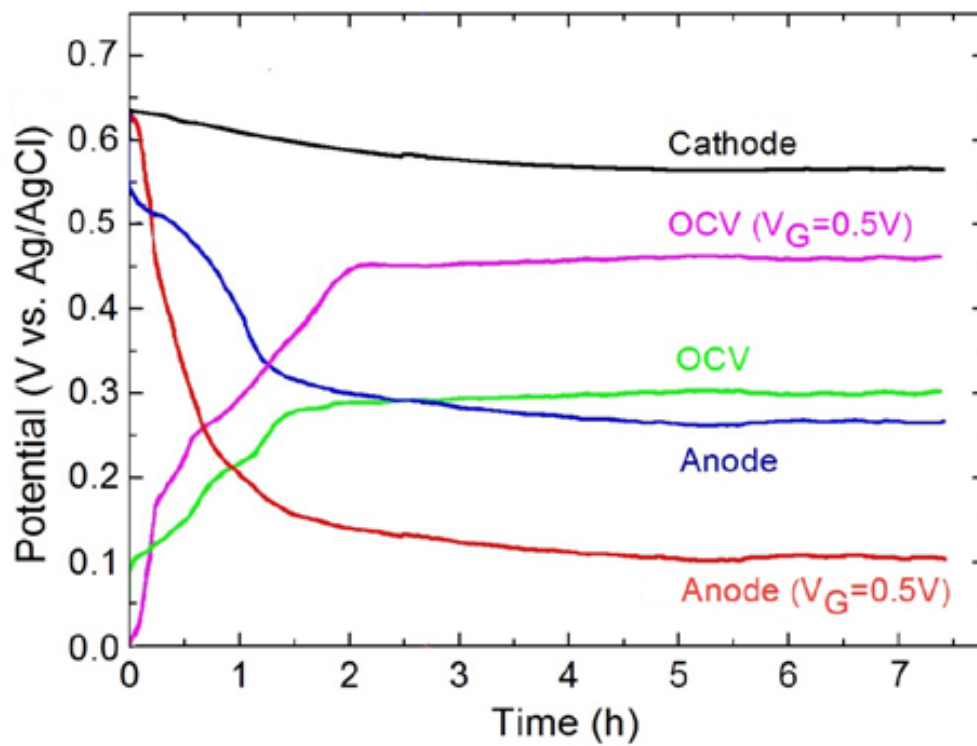


Fig 4-3 Anode potential, cathode potential and OCV

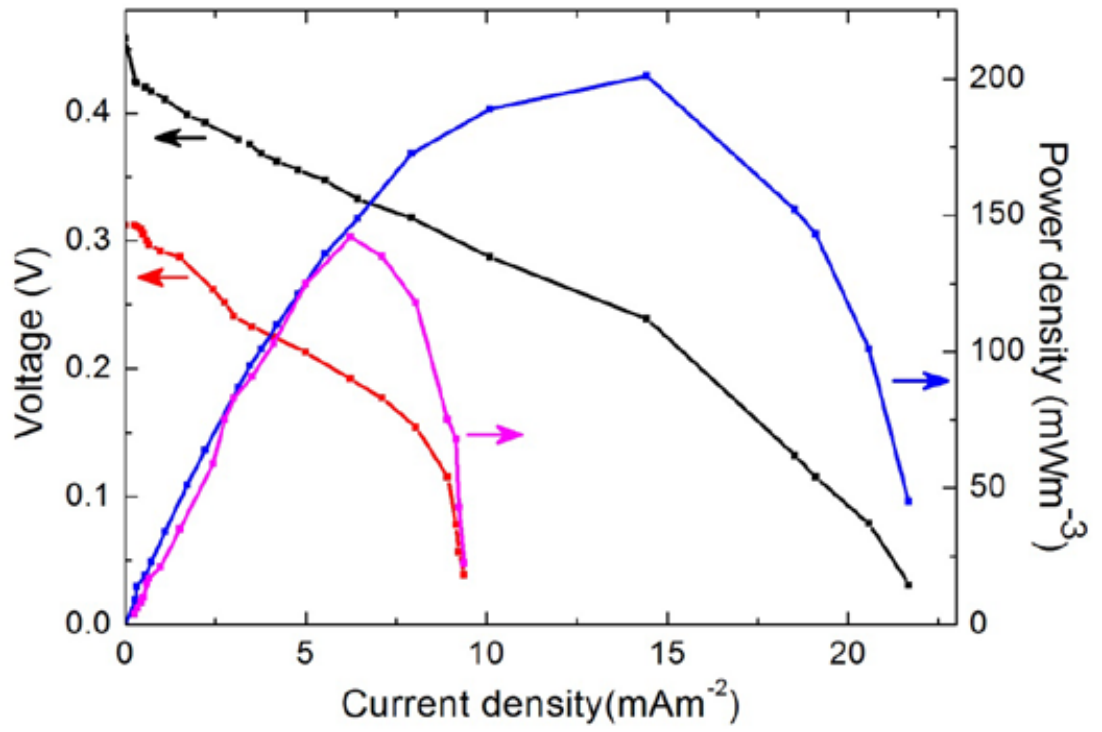


Fig 4-4 Polarization curve and power curve

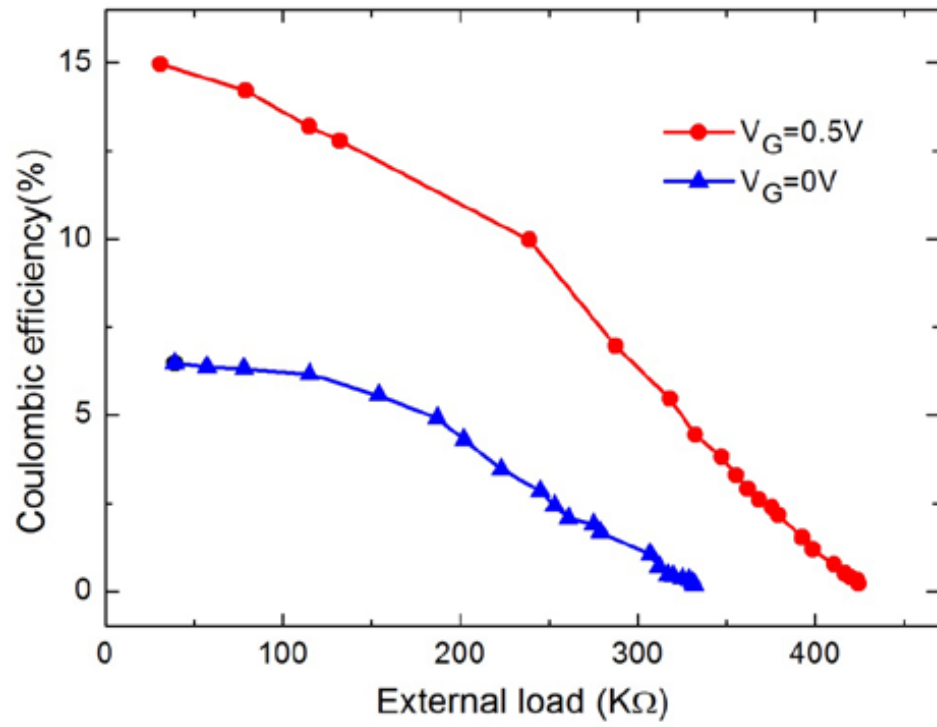


Fig 4-5 Coulombic efficiency of MFC

## **CHAPTER V**

### **CONCLUSIONS AND FUTURE WORK**

#### **5.1 Conclusions**

This thesis presents a systematic study of field-effect enzymatic detection (FEED) technique. The mechanism of the FEED has been studied. It can be predicted that FEED induced ions could set up electric field at enzyme-solution interface. FEED has been applied to the yeast-electrode system in order to show the feasibility of controlling the kinetics of cellular glucose metabolic processes at the surface of an electrode. And the FEED technique was also applied to yeast-based microbial fuel cell (MFCs) to improve its performance.

It has been verified that gating voltage ( $V_G$ ) induced ions could set up electric field at enzyme-solution interface from the observation of the  $V_G$  dependent glucose oxidation current corresponding to the ion concentration of phosphate buffer solution. The kinetics of the enzymatic conversion of glucose to gluconolactone was characterized by  $V_G$  as the parameter. And in yeast-electrode system, the glucose consumption qualitatively correlating to the production of the end products of glucose metabolism such as ethanol

and ATP indicates that the entire process was glucose metabolism whose kinetics was controlled by  $V_G$ . In yeast-MFC, FEED could increase the open circuit voltage (OCV) of cell with the range from 0.30V to 0.47V and the coulombic efficiencies (CEs) -were increased from 6% to 15%.

## 5.2 Future work

In other research field, this FEED technique can be used in cellular glucose metabolism. Glucose cellular metabolism involves redox reactions catalyzed by different kind of redox enzymes. For example, the reduction of the  $NAD^+$  to form NADH by glyceraldehyde-3-phosphate dehydrogenases in glycolysis or by alcohol dehydrogenase for maintaining redox balance of cell, either or both processes are influenced by induced electric field [1]. Our work shows a method to control cellular glucose metabolism.  $V_G$ -induced electric field can control transfer of electrons due to modulating the height of electron tunnel barrier, resulting in an enhanced glucose metabolism process. Previously, it has been demonstrated that FEED controlled electron transfer in protein could change oxidation current leading to a reorientation of cytochrome C on the electrode [2-4]. In biology research area, external controlled electron transfer had been performed [5]. By controlling electron transfer rate in metabolism system, it had been issued very most important effects [6]. The FEED technique could influence electron transfer through the cell membrane [7]. In broader sense, the technology could be applied to improve the performance of enzyme-based biosensor or bio-system.



### 5.3 References

- [1] C. K. Mathews, K. E. van Hold and K. G. Ahern, *Biochemistry*, Addison Wesley Longman, San Francisco, 1999.
- [2] Willit J L, Bowden E F. Determination of unimolecular electron transfer rate constants for strongly adsorbed cytochrome *c* on tin oxide electrodes[J]. *Journal of electroanalytical chemistry and interfacial electrochemistry*, 1987, 221(1): 265-274.
- [3] Strauss E, Thomas B, Yau S T. Enhancing electron transfer at a cytochrome *c*-immobilized microelectrode and macroelectrode[J]. *Langmuir*, 2004, 20(20): 8768-8772.
- [4] Kranich A, Ly H K, Hildebrandt P, et al. Direct observation of the gating step in protein electron transfer: Electric-field-controlled protein dynamics[J]. *Journal of the American Chemical Society*, 2008, 130(30): 9844-9848.
- [5] Heller B A, Holten D, Kirmaier C. Control of electron transfer between the L-and M-sides of photosynthetic reaction centers[J]. *Science*, 1995, 269(5226): 940-945.
- [6] Davidson V L. Chemically gated electron transfer. A means of accelerating and regulating rates of biological electron transfer[J]. *Biochemistry*, 2002, 41(50): 14633-14636.
- [7] Warshel A, Schlosser D W. Electrostatic control of the efficiency of light-induced electron transfer across membranes[J]. *Proceedings of the National Academy of Sciences*, 1981, 78(9): 5564-5568.